arXiv:1604.01491v1 [math.PR] 6 Apr 2016

ASYMPTOTICS OF RANDOM DOMINO TILINGS OF RECTANGULAR AZTEC DIAMONDS

ALEXEY BUFETOV AND ALISA KNIZEL

Abstract. We consider asymtotics of a domino tiling model on a class of domains which we call rectangular Aztec diamonds. We prove the Law of Large Numbers for the corresponding height functions and provide explicit formulas for the limit. For a special class of examples, the explicit parametrization of the frozen boundary is given. It turns out to be an algebraic curve with very special properties. Moreover, we establish the convergence of the fluctuations to the Gaussian Free Field in appropriate coordinates. Our main tool is a recently developed moment method for discrete particle systems.

1. Introduction

We study the asymptotic behavior of uniformly random domino tilings of domains drawn on the square grid. This model has received a significant attention in the last thirty years ([13], [14], [16], [21], [23], [24]). Let us briefly describe our results.

We consider a class of domains, which we call *rectangular Aztec diamonds*, see Figure 1 for an example. This type of domains generalizes a well-known case of the Aztec diamond, introduced in [16], at the same time inheriting many of its combinatorial properties. For instance, similar to the Aztec diamond, the domains we consider also have a rectangular shape with sawtooth boundary.

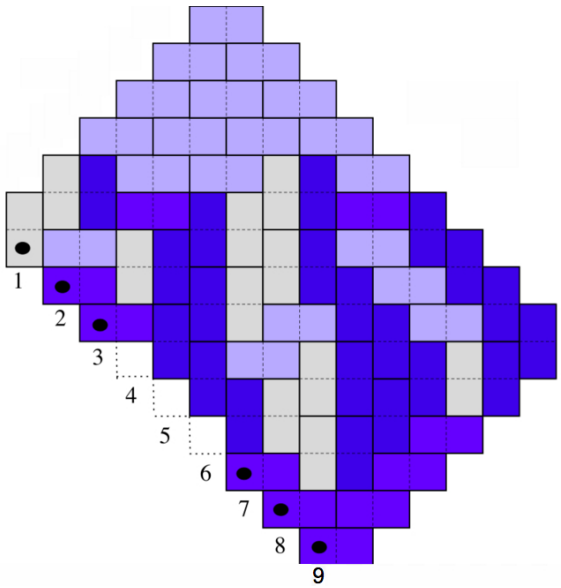

Figure 1. Domino tiling of a Rectangular Aztec diamond $\mathcal{R}(6,(1,2,3,7,8,9),3)$.

The main feature of this class of domains is a variety of different boundary conditions which are allowed on one side of the rectangle. These boundary conditions are parameterized by

boxes with dots as presented in Figure 1. When the mesh size goes to zero the limit behavior of the boundary boxes can be parameterized by a probability measure $\mathbf{m}$ with a compact support. We are able to analyze a global asymptotic behavior of the uniform random tiling of such a domain for an arbitrary choice of this measure.

Limit shape. A domino tiling can be conveniently parameterized by the so-called *height function*, see Section 3.2. It is an integer-valued function on the vertices of the square grid inside the domain, which satisfies certain conditions (see Definition 3.10 for further details). There is a one-to-one correspondence between tilings and height functions (as long as the height is fixed at one vertex). A random domino tiling naturally gives rise to a random height function. In Theorem 3.12 we prove that for an arbitrary measure $\mathbf{m}$ a random height function converges to a determenistic function, furthermore, we give an explicit formula for it.

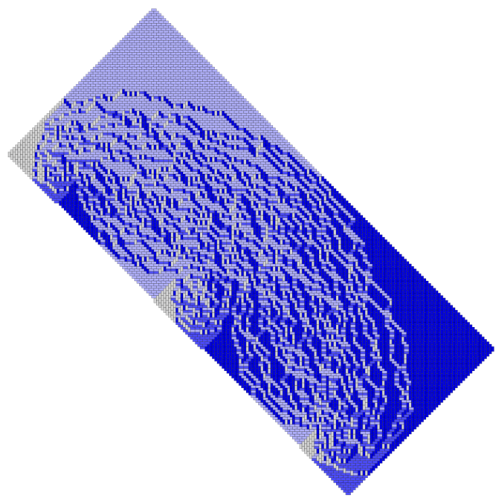

FIGURE 2. A limit shape simulation. There is a formation of brick-wall pattern in the areas near the boundary of the domain.

In [14] it was shown that the limit shape exists for a wide class of domains on the square grid and can be found as a solution to a certain variational problem. Our approach is different and provides an explicit formula for the limit function. Our computation of the limit shape is closely related to the notion of the free projection from the free probability theory (see Remark 3.9).

Frozen boundary. Typically, a limit shape forms frozen facets, that is areas, where only one type of domino is present. There also exists a connected open *liquid region* inside the domain with an arbitrary configuration of dominos. The curve, which separates the liquid region from the frozen zones is called *frozen boundary*.

In a particular case, when the measure $\mathbf{m}$ is a uniform measure of density 1 on a union of s segments, we give an explicit parametrization of the frozen boundary, see Theorem 5.1. It turns out to be an algebraic curve of rank $2s$ and genus zero with very special properties. The degree of the frozen boundary linearly depends on the number of segments. Therefore, the subclass of domains we consider provides a diverse variety of limit shapes of an arbitrary complexity.

Moreover, our formulas allow to analyze the frozen boundary for an arbitrary measure $\mathbf{m}$. We discuss several interesting examples in Section 7. The more complicated boundary

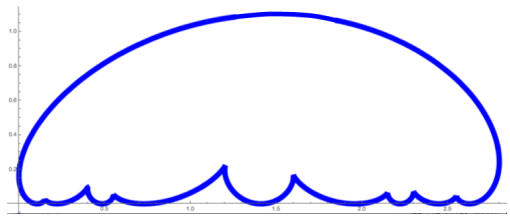

FIGURE 3. An example of the frozen boundary with $s = 5$.

conditions produce new effects; in particular, the frozen boundary is no longer an algebraic curve in a generic situation.

Fluctuations. For arbitrary boundary conditions we prove a Central Limit Theorem for a global behavior of the random height function (see Theorem 6.8), which is the main result of this paper. We show that after a suitable change of coordinates the fluctuations are described by the *Gaussian Free Field*. The appearence of the Gaussian free field as a universal object in this class of probabilistic tiling models originates from the work of Kenyon (see [24], [25]).

In [24] Kenyon proved a central limit theorem for uniformly random tilings of domains of an arbitrary shape, but with very special boundary conditions. In contrast, we analyze the rectangular domains, but with arbitrary boundary conditions on one of the sides. Depending on the boundary conditions, the Law of Large Numbers can have a quite complicated form. It is reflected in a (possibly complicated) choice of the *complex structure*, that is a map from the liquid region into the complex half-plane. In other words, it is the choice of the coordinate in which the Gaussian Free Field appears as a limit object.

A parallel (and actually more developed) story exists for the case of *lozenge* tilings. We refer to [26] for the exposition and further references on the subject. Both the domains we consider and the fluctuation results are close in spirit to [31], [32], however, the approach we take is entirely different.

We use a moment method for this type of problems. It was introduced and developed in [7], [8]. Let us comment on two known methods. The method based on the study of a family of orthogonal polynomials, which was extensively used in the case of the Aztec diamond, does not seem to be available in our setting. The results in [31], [32] as well as in [15], rely on the explicit computation of the correlation kernel of the corresponding determinantal process. The process that we study is similar to a Schur process, however, it is an important challenge to find a reasonable correlation kernel of such a process and to perform its asymptotic analysis. We believe that the moment method is the most suitable method for the analysis of the global behavior in this class of problems (see Remark 6.9 for further comments).

In this paper we give a "model case" analysis of a specific class of domino tilings. However, we believe that the moment method and the tools developed in this paper are applicable in many other models. Let us mention some of them.

The domino tiling model considered in this paper can be interpreted as a random collection of non-intersecting lines, see Figure 4 and Section 2.3 for details. In the case of the Aztec diamond this interpretation was first used by Johansson in [22], and later many similar and more general ensembles of non-intersecting lines were studied, see [3], [4], [5], [6] and

references therein. Some of these ensembles can be viewed as dimer models. More precisely, in [6] it was shown how to interpret an arbitrary Schur process as a dimer model on a rail yard graph.

The main novelty of the presented approach is that we consider non-intersecting lines with *arbitrary* boundary conditions on one side. We suggest that all the models above can be analyzed with the use of the moment method and the results of this paper. Because the global behavior of the height function significantly depends on the boundary conditions in all these models, we expect further interesting results in this direction.

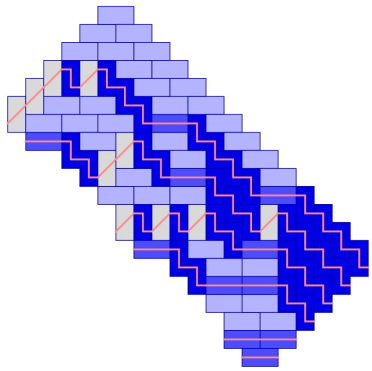

FIGURE 4. Rectangular Aztec diamond $\mathcal{R}(6,(1,2,4,5,7,8),12)$ and the corresponding set of non-intersecting lines.

Acknowledgements. The authors are deeply grateful to Alexei Borodin and Vadim Gorin for very helpful discussions.

2. The model description

2.1. **Combinatorics of the model.** Let us present a formal definition of the domain we are considering.

Definition 2.1. *Let $N \in \mathbb{N}$ and $\Omega = (\Omega_1, \dots, \Omega_N)$, where $1 = \Omega_1 < \Omega_2 < \dots < \Omega_N$ and $\Omega_i \in \mathbb{N}$. Set $m = \Omega_N - N$.*

Introduce the coordinates (i,j) as in Figure 5. Let us denote by $C(i,j)$ a unit square with the vertex coordinates (i,j), $(i-\frac{1}{2}, j+\frac{1}{2})$, $(i+\frac{1}{2}, j+\frac{1}{2})$, $(i, j+1)$.

The rectangular Aztec diamond $\mathcal{R}(N,\Omega,m)$ is a polygonal domain which is built of $2N+1$ rows of unit squares $C(i,j)$. Let us enumerate the rows starting from the bottom as shown in Figure 5. Then the k-th row consists of unit squares $C(i,j)$, where

- *$i = 0, 1, \dots, \Omega_N$ and $j = 0, 1, \dots, N-1$, when $k = 2i$, $i = 0, 1, \dots, N$;*
- *$i = \frac{1}{2}, \frac{3}{2}, \dots, \Omega_N - \frac{1}{2}$ and $j = \frac{1}{2}, \frac{3}{2}, \dots, N - \frac{1}{2}$, when $k = 2i+1$, $i = 1, 2, \dots, N$;*
- *$i = \Omega_l - \frac{1}{2}$ and $j = -\frac{1}{2}$ for $l = 1, 2, \dots, N$, when $k = 1$. We call this row the boundary of $\mathcal{R}(N,\Omega,m)$.*

Definition 2.2. *A domino tiling of a rectangular Aztec diamond $\mathcal{R}(N,\Omega,m)$ is a set of pairs $(C(i_1,j_1), C(i_2,j_2))$, called dominos, such that the unit squares $C(i_1,j_1), C(i_2,j_2) \subset \mathcal{R}(N,\Omega,m)$ share an edge.*

Let us denote the set of domino tilings of $\mathcal{R}(N,\Omega,m)$ by $\mathfrak{D}(N,\Omega,m)$.

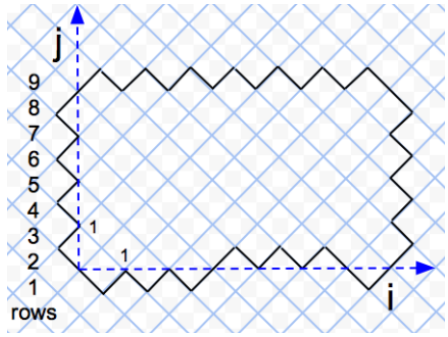

FIGURE 5. Rectangular Aztec dimond $\mathcal{R}(4, \Omega = (1, 2, 3, 7), 3)$.

Definition 2.3. *Let $D \in \mathfrak{D}(N, \Omega, m)$ be a domino tiling of $\mathcal{R}(N, \Omega, m)$. We call a domino $d = (C(i_1, j_1), C(i_2, j_2)) \in D$ a V-domino if $max(i_1, i_2) \in \mathbb{N}$ and we call it a Λ-domino otherwise. In other words, the dominos going upwards starting from an odd row are V-dominos and those ones starting from an even row are Λ-dominos. We also call the corresponding squares $C(i_1, j_1), C(i_2, j_2)$ — V-squares and Λ-squares accordingly.*

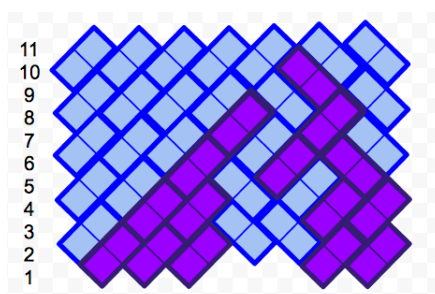

FIGURE 6. Domino tiling of $\mathcal{R}(4, \Omega = (1, 2, 3, 7), 3)$. The V-squares are purple and Λ-squares are blue.

Lemma 2.4. *The set of V-squares in $\mathcal{R}(N, \Omega, m)$ determines the tiling uniquely.*

Proof. Let us reconstruct the tiling given the set of V-squares coming from some unknown tiling. We will show that we can reconstruct it in a unique way. Let us enumerate the squares in each row from left to right.

We start by looking at the V-squares in the first row. All squares in the first row are V-squares and there are exactly N of them. Let us take the first V-square in the first row. We will pair it with the first V-square in the second row. We can always do it since we know that there exists at least one domino tiling with this set of V-squares. We can proceed until the end of the first row. Note that at this point we have used all V-squares from the second row and this is the only way we could pair the V-squares from the first row with something.

Now we pair the first Λ-square in the second row with the first Λ-square in the third row. We can proceed until the end of the second row. Note that at this point we have used all squares from the second row and all Λ-squares from the third row. Moreover, this is the only way we could pair Λ-squares from the second row with something. Now we look at V-squares in the third row and notice that there are $N - 1$ of them. This is because the total number of squares in the third row is less by one than the total number of squares in the second row. We start pairing them with V-squares from the third row in the same way.

We continue in this fashion until we pair all Λ-squares from row $2N$ with all the squares from row $2N+1$.

$\square$

Definition 2.5. *Let μ be a n-tuple of natural numbers $\mu = (\mu_1 \geqslant \mu_2 \cdots \geqslant \mu_n \geqslant 0)$. We will denote $|\mu| = n$. A Young diagram Y_μ is a set of boxes in the plane with μ_1 boxes in the first row, μ_2 boxes in the second row, etc.*

We call a Young diagram Y_μ rectangular $n \times m$ Young diagram if $m = \mu_1 = \mu_2 = \cdots = \mu_n$. Let us denote it $Y_{n\times m}$.

Definition 2.6. *Let Y_μ be a Young diagram, where $\mu = \mu_1 \geqslant \mu_2 \cdots \geqslant \mu_n \geqslant 0$. A dual Young diagram $Y_{\mu^\vee}$ is obtained by flipping the original diagram Y_μ about its diagnal. Explicitly we have that $\mu_i^\vee$ is equal to the length of the i-th column of Y_μ.*

Construction 2.7. *Due to Lemma 2.4 we can encode any domino tiling $D \in \mathfrak{D}(N, \Omega, m)$ pictorially as it is shown in Figure 7. We simply put a yellow node in the center of every V-square from an even row and a pink node in the center of every V-square from an odd row. The configuration of these nodes determines the tiling uniquely. In the case of the Aztec diamond such encoding was suggested by Johansson* [22].

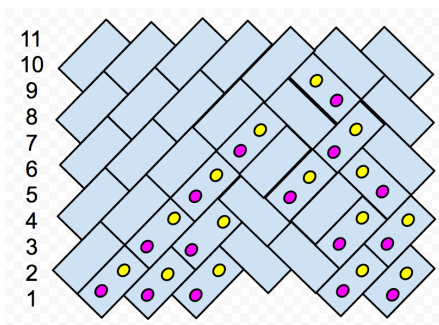

FIGURE 7. An example of a domino tiling of $\mathcal{R}(5, \Omega = (1,2,3,6,7), 3)$. We put nodes in the centers of V-squares.

Let us associate to every configuration of the nodes the following sequence of Young diagrams Y_j. Each diagram Y_j corresponds to the j-th row $j = 1, 2, \ldots, 2N$, which has n_j V-squares and m_j Λ-squares. Let us take a rectangular $n_j \times m_j$ Young diagram. We start drawing a stepped line ℓ_j inside it starting from the left bottom corner. At step k if the i-th square in the row is a V-square ℓ_j goes up by one, otherwise the line goes to the right by one. The stepped line ℓ_j is the boundary of a Young diagram, see Figure 8.

Let us look at the j-th row. It has $N - \lfloor \frac{j-1}{2} \rfloor$ V-squares in positions $i_1, \ldots, i_{N-\lfloor \frac{j-1}{2} \rfloor}$ starting from the left. Then the Young diagram we obtain corresponds to the $N - \lfloor \frac{j-1}{2} \rfloor$-tuple $(i_{N-\lfloor \frac{j-1}{2} \rfloor} - \lfloor \frac{j-1}{2} \rfloor, \ldots, i_1 - 1)$.

To construct a Young diagram corresponding to the boundary row we complete the row by virtually adding m Λ-squares so that $\mathcal{R}(N, \Omega, m)$ becomes a proper rectangular with sawtooth boundary. Let us denote the Young diagram corresponding to the boundary row Y_ω, where ω is an N-tuple of integers, more precisely, $\omega = (\Omega_N - N, \ldots, \Omega_1 - 1)$.

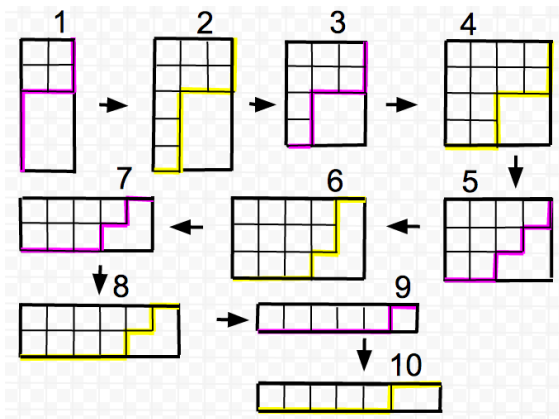

FIGURE 8. A sequence of Young diagrams corresponding to the domino tiling $\mathcal{R}(5, \Omega = (1, 2, 3, 6, 7), 3)$ presented in Figure 7.

Definition 2.8. *Let Y_ω, where $\omega = \omega_1 \geqslant \omega_2 \cdots \geqslant \omega_N \geqslant 0$, be a Young diagram contained in a rectangular $N \times m$ Young diagram $Y_{N\times m}$. Let $\mathcal{S}(Y, N, m)$ be the following set of sequences of Young diagrams*

$$\mathcal{S}(Y_\mu, N, m) = \{(Y_{\mu^{(N)}} = Y_\omega, Y_{\nu^{(N)}}, \ldots, Y_{\mu^{(1)}}, Y_{\nu^{(1)}}\},$$

such that

- $|\mu^{(i)}| = i$ *and* $|\nu^{(i)}| = i$ *for* $i = 1, 2, \ldots, N$.
- $Y_{\mu^{(i)}} \subset Y_{i\times(m+N-i)}$ *for* $i = 1, 2, \ldots, N$;
- $Y_{\nu^{(i)}} \subset Y_{i\times(m+N-i+1)}$ *for* $i = 1, 2, \ldots, N$;
- $Y_{\mu^{(i)}} \subset Y_{\nu^{(i)}}$ *for* $i = 1, 2, \ldots, N$;
- $Y_{\nu^{(i)}} \setminus Y_{\mu^{(i)}}$ *is a vertical strip of length* $l \leqslant i$ *for* $i = 1, 2, \ldots, N$; *that is* $Y_{\nu^{(i)}}$ *can be obtained from* $Y_{\mu^{(i)}}$ *by adding* l *boxes, no two in the same row, see Figure 9.*
- $Y_{\nu^{(i+1)}} \backslash Y_{\mu^{(i)}}$ *is a horizontal strip. In other words, they interlace* $(Y_{\mu^{(i)}} \prec Y_{\nu^{(i+1)}})$, *that is*

$$\nu_1^{(i+1)} \geqslant \mu_1^{(i)} \geqslant \cdots \geqslant \nu_i^{(i+1)} \geqslant \mu_i^{(i)} \geqslant \nu_{i+1}^{(i+1)}, \text{ for } i = 1, 2, \ldots, N-1.$$

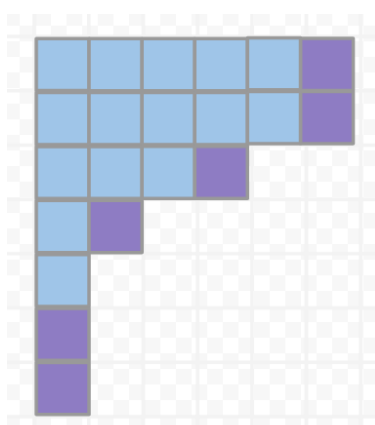

FIGURE 9. Purple boxes form a vertical strip of length 6.

Theorem 2.9. *The Construction 2.7 defines a map*

$$Y\colon \mathfrak{D}(N,\Omega,m) \to \mathcal{S}(Y_\omega, N, m).$$

The map is bijective.

Proof. Let $\mathcal{D} \in \mathfrak{D}(N,\Omega,m)$ be a domino tiling and let $Y(\mathcal{D}) = (Y_{\mu^{(n)}=\omega}, Y_{\nu^{(N)}}, \dots, Y_{\mu^{(1)}}, Y_{\nu^{(1)}})$. Let us first check that this map is well-defined, i.e. $Y(\mathcal{D}) \in \mathcal{S}(Y_\omega, N, m)$. Thus, we need to verify all the properties 2.8.

- By construction $Y_{\mu^{(i)}} \subset Y_{n_i \times m_i}$, where n_i and m_i are the number of V-squares and Λ-squares in the row with number $2(N-i)+1$. Following the proof of Lemma 2.4 we see that $n_i = i$ and $m_i = N+m-i$. Also, the length of $Y_{\mu^{(i)}}$ is equal to the number of V-squares in the corresponding row. Thus, we get $|\mu^{(i)}| = i$. Similarly we have $Y_{\nu^{(i)}} \subset Y_{i\times(m+N-i+1)}$ and $|\nu^{(i)}| = i$.
- Note that by construction $\mu_j^{(i)}$ is precisely the number of Λ-squares to the left from the j-th V-square in the corresponding row with number $k = 2(N-i)+1$. Let us look at this row. The V-squares from it are paired with V-squares from the next row in $\mathcal{D}$. It can be shown by induction that the number of Λ-squares to the left from the j-th V-square in the $k+1$ row is always equal or grater by one than the same quantity for the j-th V-square in the k-th row. It follows from the fact that if the j-th V-square is in position n in the k-th row (i.e. it is the n-th square from the left in this row) it must be paired with the j-th V-square from the next row in position n or $n+1$, see Figure 6. Therefore, $Y_{\mu_j^{(i)}} \subset Y_{\nu_j^{(i)}}$ and $Y_{\nu^{(i)}} \setminus Y_{\mu^{(i)}}$ is a vertical strip with a number of blocks $\leqslant i$.
- Consider $Y_{\nu^\vee,(i)}$, the Young diagram dual to $Y_{\nu^{(i)}}$. Note that by construction $\nu_j^{\vee,(i)}$ is precisely the number of V-squares to the left from the j-th Λ-square in the corresponding row with number $k = 2(N-i)+2$, where this time we count from the right. Let us look at this row. Then the Λ-squares from the next row are paired with the Λ-squares from this row, moreover, the j-th Λ-square in position n is paired with the j-th Λ-square in position n or $n+1$ from the next row counting from the right. Again, we get that $Y_{\nu^\vee,(i)} \setminus Y_{\mu^\vee,(i+1)}$ is a vertical strip. Thus, $Y_{\mu^{(i+1)}} \setminus Y_{\nu^{(i)}}$ is a horizontal strip. Therefore, the interlacing condition holds.

So far we have checked that the map Y is well-defined. From Lemma 2.4 it follows that it is injective.

Let us construct the inverse map $Y^{(-1)}\colon \mathcal{S}(Y_\alpha, N, m) \to \mathfrak{D}(N,\Omega,m)$. Inverting the Construction 2.7 we see that each element $y \in \mathcal{S}(Y_\alpha, N, m)$ defines a configuration of V-squares. Our goal is to show that there exists a tiling with such a configuration of V-squares. We can reconstruct it using the same ideas as we used in the proof of Lemma 2.4. We start by pairing V-squares from the first row with V-squares from the second row starting from the left. We can always pair the j-th V-square from the first row in position n with the i-th V-square from the second row because it has to be in position n or $n+1$ due to our assumptions on y. Then we proceed to the next row and pair Λ-squares with Λ squares in the third row. The map $Y^{(-1)}$ is then well-defined and injective. Therefore, Y is a bijection. □

2.2. **Uniform measure on $\mathcal{S}(Y_\alpha, N, m)$.** Theorem 2.9 allows us to reduce any question about the uniform measure on the set of domino tilings $\mathfrak{D}(N,\Omega,m)$ to the same question for the uniform measure on $\mathcal{S}(Y_\alpha, N, m)$. This is the core of our approach.

Let $U(N)$ denote the group of all $N \times N$ complex unitary matrices. It is well-known that all irreducible representations of $U(N)$ are parameterized by their highest weights, which are *signatures* of length N— N-tuples of integers $\lambda = (\lambda_1 \geqslant \lambda_2 \geqslant \cdots \geqslant \lambda_N)$. We denote by $\mathbb{GT}_N$ the set of all signatures and the length of a signature is denoted by $|\lambda|$. We call a signature *non-negative* if $\lambda_N \geqslant 0$. Note that the set of all nonnegative signatures $\mathbb{GT}_N^+$ is in bijection with the set of Young diagrams $\mathbb{Y}$ with N rows (rows are allowed to have zero length).

Definition 2.10. *Let $\lambda \in \mathbb{GT}_N$. The rational Schur function is*

$$s_\lambda(u_1, \ldots, u_N) = \frac{\det_{i,j=1,\ldots,N}(u_i^{\lambda_j+N-j})}{\prod\limits_{1\leqslant i<j\leqslant N}(u_i - u_j)}. \tag{2.1}$$

Proposition 2.11. (*Weyl,* [36]) *The value of the character of the irreducible representation π^λ corresponding to the signature $\lambda = (\lambda_1 \geqslant \cdots \geqslant \lambda_N)$ on a unitary matrix $\mathfrak{u} \in U(N)$ with eigenvalues $u_1, \ldots, u_n$ is given by the rational Schur function:*

$$\mathrm{Trace}(\pi^\lambda(\mathfrak{u})) = s_\lambda(u_1, \ldots, u_N).$$

Let $\mu^{(n)}$ and $\nu^{(n)}$ be two non-negative signatures of length n. Recall that Schur functions form a basis for the algebra of symmetric functions. Define the coefficients $\mathrm{st}(\mu^{(n)} \to \nu^{(n)})$ and $\mathrm{pr}(\nu^{(n)} \to \mu^{(n-1)})$ via

$$\frac{s_{\mu^{(n)}}(u_1, \ldots, u_n)}{s_{\mu^{(n)}}(1^n)} \prod_{i=1}^n \frac{(1+u_i)}{2} = \sum_{\nu^{(n)}\in\mathbb{GT}_n} \mathrm{st}(\mu^{(n)} \to \nu^{(n)}) \frac{s_{\nu^{(n)}}(u_1, \ldots, u_n)}{s_{\nu^{(n)}}(1^n)}, \tag{2.2}$$

$$\frac{s_{\nu^{(n)}}(u_1, \ldots, u_{n-1}, 1)}{s_{\nu^{(n)}}(1^n)} = \sum_{\mu^{(n-1)}\in\mathbb{GT}_{n-1}} \mathrm{pr}(\nu^{(n)} \to \mu^{(n-1)}) \frac{s_{\mu^{(n-1)}}(u_1, \ldots, u_n)}{s_{\mu^{(n-1)}}(1^n)}, \tag{2.3}$$

where 1^n is a notation for a string $(1, 1, \ldots, 1)$ of length n.

Lemma 2.12. *The following equalities hold*

$$\sum_{\nu^{(n)}\in\mathbb{GT}_n} \mathrm{st}(\mu^{(n)} \to \nu^{(n)}) = 1 \text{ and } \sum_{\mu^{(n-1)}\in\mathbb{GT}_{n-1}} \mathrm{pr}(\nu^{(n)} \to \mu^{(n-1)}) = 1. \tag{2.4}$$

Proof. Our goal is to explicitly compute $\mathrm{st}(\mu^{(n)} \to \nu^{(n)})$ and $\mathrm{pr}(\nu^{(n)} \to \mu^{(n-1)})$. Let us start with the first one. Let e_l be the l-th elementary symmetric function. Recall the Pieri's rule

$$e_l s_\mu = \sum_{\mu\subset\lambda} s_\lambda,$$

where the sum is taken over λ obtained from μ by adding l boxes, no two in the same row.

Note that

$$\prod_{j=1}^n \frac{1+u_j}{2} = \frac{1}{2^n} \sum_{j=1}^n e_j(u_1, \ldots, u_n).$$

Therefore,

$$\mathrm{st}(\mu^{(n)} \to \nu^{(n)}) = \begin{cases} \frac{s_{\nu^{(n)}}(1^n)}{2^n s_{\mu^{(n)}}(1^n)}, & \mu^{(n)} \subset \nu^{(n)}; \\ 0, & \textit{otherwise}, \end{cases} \tag{2.5}$$

where $\nu^{(n)}$ is obtained from $\mu^{(n)}$ by adding l boxes such that $l \leqslant n$.

We can also compute

$$s_{\mu^{(n)}}(1^n)e_l(1^n) = s_{\mu^{(n)}}(1^n)\binom{n}{l} = \sum_{\mu^{(n)}\subset\lambda} s_\lambda(1^n), \tag{2.6}$$

where the sum is taken over λ obtained from $\mu^{(n)}$ by adding l boxes, no two in the same row.

From (2.6) we conclude

$$\sum_{\nu^{(n)}\in\mathbb{GT}_n} \mathrm{st}(\mu^{(n)} \to \nu^{(n)}) = \frac{1}{2^n}\sum_{l=1}^{n}\binom{n}{l} = 1.$$

The equation (2.3) is a well-known branching rule for the Schur polynomials. Thus, we get

$$\mathrm{pr}(\nu^{(n)} \to \mu^{(n-1)}) = \begin{cases} \frac{s_{\mu^{(n)}}(1^n)}{s_{\nu^{(n)}}(1^n)}, & \mu^{(n-1)} \prec \nu^{(n)}; \\ 0, & \textit{otherwise}. \end{cases} \tag{2.7}$$

Moreover, we have

$$\dim(\pi^{\mu^{(n)}}) = s_{\mu^{(n)}}(1^n) = \sum_{\nu^{(n)}\prec\mu^{(n)}} \dim(\pi^{\nu^{(n)}}) = \sum_{\nu^{(n)}\prec\mu^{(n)}} s_{\nu^{(n)}}(1^n).$$

Thus, the second equality also holds. □

Let us fix a signature μ of length N. Lemma 2.12 allows us to define the probability measure on the sequences of signatures of the form

$$\mathcal{S}^N = \{(\mu^{(N)}, \nu^{(N)}, \dots, \mu^{(1)}, \nu^{(1)})\}$$

by the formula

$$\begin{aligned} &\mathcal{P}^N_\mu((\mu^{(N)}, \nu^{(N)}, \dots, \mu^{(1)}, \nu^{(1)})) = \\ &\quad = 1_{\mu^{(N)}=\mu}\mathrm{st}(\mu^{(N)} \to \nu^{(N)}) \prod_{j=1}^{N-1}(\mathrm{pr}(\nu^{(N-j+1)} \to \mu^{(N-j)})\mathrm{st}(\mu^{(N-j)} \to \nu^{(N-j)})), \end{aligned} \tag{2.8}$$

where $\mu^{(i)}, \nu^{(i)} \in \mathbb{GT}_i$.

Proposition 2.13. *Let $\mathcal{R}(\Omega, N, m)$ be a rectangular Aztec diamond. Let us denote the support of measure $\mathcal{P}^N_\omega$ by $\mathbb{S}_\omega$, where ω is the signature corresponding to the boundary row of $\mathcal{R}(\Omega, N, m)$. The set of domino tilings $\mathfrak{D}(\Omega, N, m)$ of $\mathcal{R}(\Omega, N, m)$ is in bijection with $\mathbb{S}_\omega$. Moreover, the measure $\mathcal{P}^N_\omega$ is uniform on $\mathbb{S}_\omega$ and, therefore, on $\mathfrak{D}(\Omega, N, m)$.*

Proof. From (2.7) and (2.5) for any $(\mu^{(N)}, \nu^{(N)}, \dots, \mu^{(1)}, \nu^{(1)})$ we have

$$\begin{aligned}
&\mathcal{P}^N_\omega(\mu^{(N)}, \nu^{(N)}, \dots, \mu^{(1)}, \nu^{(1)})) = \\
&= \frac{1}{2^N} \frac{s_{\nu^{(1)}}(1^N)}{s_{\mu^{(1)}}(1^N)} \frac{s_{\mu^{(2)}}(1^{N-1})}{s_{\nu^{(1)}}(1^N)} \frac{1}{2^{N-1}} \frac{s_{\nu^{(2)}}(1^{N-1})}{s_{\mu^{(2)}}(1^{N-1})} \cdots \frac{1}{2} \frac{s^{\nu^{(N)}}(1)}{s_{\mu^{(N)}}(1)} = \\
&= \frac{1}{2^{N(N+1)/2} s_\omega(1^N)},
\end{aligned}$$

when $(\mu^{(N)}, \nu^{(N)}, \dots, \mu^{(1)}, \nu^{(1)}) \in \mathcal{S}(Y_\omega, N, m)$ and zero otherwise. Recall that by Theorem 2.9 the set $\mathcal{S}(Y_\omega, N, m)$ is in bijection with the set of domino tilings $\mathfrak{D}(\Omega, N, m)$.

Therefore, $\mathcal{P}^N_\omega$ defines the uniform measure on $\mathfrak{D}(\Omega, N, m)$.

□

Corollary 2.14. *The number of domino tilings of $\mathcal{R}(\Omega, N, m)$ is equal to*

$$|\mathfrak{D}(\Omega, N, m)| = 2^{N(N+1)/2} s_\omega(1^N). \tag{2.9}$$

This formula was obtained in [12] based on the results from [11] and [28].

2.3. **Ensembles of non-intersecting paths.** Let us describe in more detail another combinatorial interpretation of our tiling model, which was discussed in the introduction.

Superimposing a rectangular Aztec diamond upon a checkerboard coloring (the choice is irrelevant) we obtain four types of dominos, as the black unit square might be either to the right/left (resp. top/bottom) unit square of a horizontal (resp. vertical) domino. In this way to each tiling one can bijectively associate a set of non-intersecting lines, as shown in Figure 4. This construction first appeared in [22], we use a slightly different but equivalent representation from [4].

Next, one can think of a rectangular Aztec diamond as being embedded into tilings of $\mathbb{R}$, where outside the domain we add only non-overlaping horizontal dominos and fill the whole space with them.

Then, by means of a simple transformation one obtains a bijection between a tiling of a rectangular Aztec diamond $\mathcal{R}(N, \Omega, m)$ and a configuration of non-intersecting lines on a Lindström-Gessel-Viennot (LGV) directed graph (see [17] and [34]), built out of $N+m$ basic blocks, see Figure 10.

Note that Ω determines the boundary conditions on the left side as shown in Figure 10. By construction from a yellow vertex a line can go up-right or to the right, while from a red vertex the line goes to the right or down-right.

Introduce the coordinate system as in the right picture in Figure 10. Let us associate to every vertical section $t = i$, where $i = 1, \dots 2N+1$, a signature. Consider the set of nodes on a section. Suppose the nodes that belong to the lines from the ensemble have coordinates $s_1 > s_2 > \dots > s_i$. Then the corresponding signature is $(s_1 + 1 \geqslant s_2 + 2 \geqslant \dots \geqslant s_i + i)$. In this way to every non-intersecting line ensemble one associates a sequence of signatures $(\gamma_1, \rho_1, \dots, \gamma_N, \rho_N, \gamma_{N+1})$. Note that $\gamma_{N+1} = (0 \geqslant 0 \geqslant \dots \geqslant 0)$.

Consider the following probability model on the set of the non-intersecting line ensembles. Let us assign weight 1 to each horizontal edge, weight $\alpha = 1$ to each vertical edge and $\beta = \frac{1}{2}$ to each down-right edge. Consider the i-th basic block, let $(\gamma_i, \rho_i, \gamma_{i+1})$ be a triple of

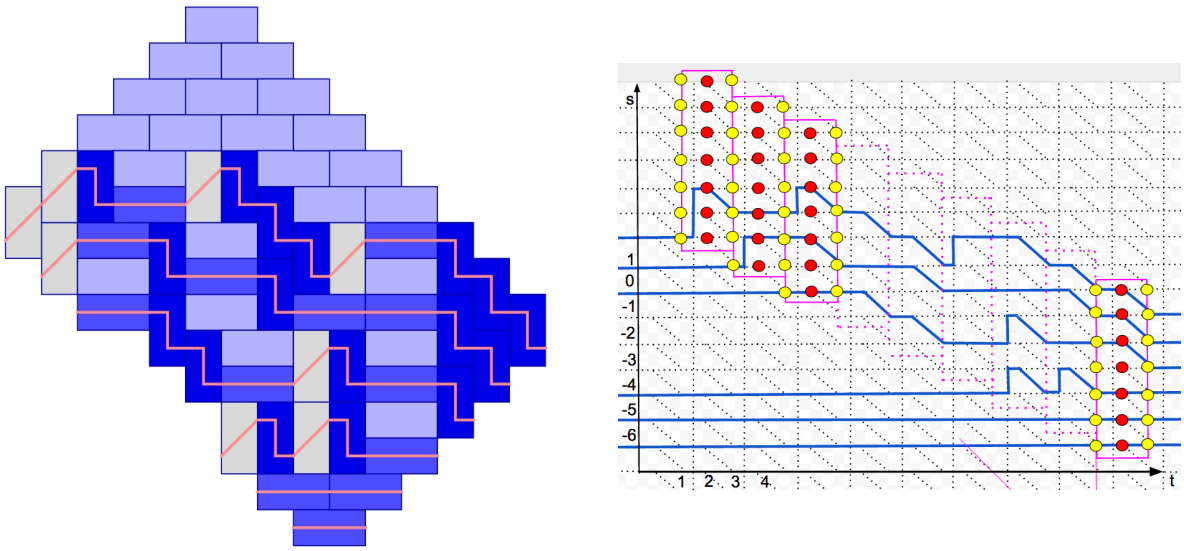

FIGURE 10. Recatangular Aztec diamond $\mathcal{R}(6,(1,2,3,7,8,9),3)$ and the corresponding ensemble of non-intersecting paths. The height of a block is $N+1$ units.

signatures corresponding to its left side, middle section and its right side. Let us assign to this block the following weight

$$w(\text{block}) = s_{\rho_i/\gamma_{i+1}}(\alpha) \cdot s_{\rho_i/\gamma_i}(\hat{\beta}).$$

Here α stands for the specialization of the symmetric functions into a single nonzero variable equal to α (with complete homogeneous symmetric functions specializing into $h_n(\alpha) = \alpha^n, n \geqslant 0$), and $\hat{\beta}$ stands for the specialization into a single 'dual' variable equal to β (with complete homogeneous symmetric functions specializing into $h_n(\hat{\beta}) = 1$ if $n = 0$, $h_n(\hat{\beta}) = \beta$ if $n = 1$, and $h_n(\hat{\beta}) = 0$ if $n \geqslant 2$).

Define the probability $\mathbb{P}_L$ of an non-intersecting line ensembles satisfying our combinatorial and boundary conditions to be the product of the corresponding weights of the blocks.

Proposition 2.15. *Measure $\mathbb{P}_L$ is a uniform probability measure on the set $L(N,\Omega,m)$ of all non-intersecting line ensembles satisfying our combinatorial and boundary conditions.*

We do not go into details of the proof of this proposition since we will not need it further, see the recent exposition in [2].

We conclude that the uniform measure on the set of tilings $\mathfrak{D}(N,\Omega,m)$ corresponds under the above bijection to a measure $\mathbb{P}_L$ on the ensembles of non-intersecting lines.

There are many other intersting tiling models that have an interpretation as ensembles of non-intersecting lines. For example, random tilings of a tower, discussed in [4]. More generally, the random dimer model on a rail yard graph [6] fits into the framework of the Schur generating functions. We believe that our approach can be used to analyze the global behavior for these models with arbitrary boundary conditions.

3. Law of Large numbers

3.1. **Preliminaries.** One way to encode a signature $\lambda \in \mathbb{GT}_N$ is through the *counting measure* $m[\lambda]$ corresponding to it via

$$m[\lambda] = \frac{1}{N}\sum_{i=1}^{N} \delta\left(\frac{\lambda_i + N - i}{N}\right). \tag{3.1}$$

Note that we incorporate the scaling into this formula.

Let ρ be a probability measure on the set of all signatures $\mathbb{GT}_N$. The push-forward of ρ with respect to the map $\lambda \to m[\lambda]$ defines a *random* probability measure on $\mathbb{R}$ that we denote $m[\rho]$.

Definition 3.1. *Let ρ be a probability measure on $\mathbb{GT}_N$. The Schur generating function $\mathcal{S}_\rho^{U(N)}(u_1, \dots, u_N)$ is a symmetric Laurent power series in $(u_1, \dots, u_N)$ given by*

$$\mathcal{S}_\rho^{U(N)}(u_1, \dots, u_N) = \sum_{\lambda \in \mathbb{GT}(N)} \rho(\lambda) \frac{s_\lambda(u_1, \dots, u_N)}{s_\lambda(1, \dots, 1)}. \tag{3.2}$$

We will need the following two results from [7].

Theorem 3.2. ([7], *Theorem 5.1*) *Let $\rho(N)$ be a sequence of measures such that for each $N = 1, 2, \dots,$ $\rho(N)$ is a probability measure on $\mathbb{GT}_N$. Suppose that $\rho(N)$ is such that for every j*

$$\lim_{N\to\infty} \frac{1}{N} \ln(\mathcal{S}_{\rho(N)}^{U(N)}(u_1, \dots, u_j, 1^{N-j})) = Q(u_1) + \dots + Q(u_j),$$

where Q is an analytic function in a neighborhood of 1 and the convergence is uniform in an open (complex) neighborhood of $(1, \dots, 1)$. Then random measures $m[\rho(N)]$ converge as $N \to \infty$ in probability, in the sense of moments to a deterministic *measure $\mathbf{m}$ on $\mathbb{R}$, whose moments are given by*

$$\int_{\mathbb{R}} x^j \mathbf{m}(dx) = \sum_{\ell=0}^{j} \frac{j!}{\ell!(\ell+1)!(j-\ell)!} \frac{\partial^\ell}{\partial u^\ell} \left(u^j Q'(u)^{j-l}\right)\Big|_{u=1}. \tag{3.3}$$

Let us introduce some notation. Let $\mathbf{m}$ be a compactly supported measure on $\mathbb{R}$. Let $M_k(\mathbf{m}) = \int_{\mathbb{R}} x^k \mathbf{m}(dx)$ be its k-th moment. Set

$$S_{\mathbf{m}}(z) = z + M_1(\mathbf{m})z^2 + z^3 M_2(\mathbf{m}) + \dots$$

to be the generating function of the moments of $\mathbf{m}$. Define $S_{\mathbf{m}}^{(-1)}(z)$ to be the inverse series to $S_{\mathbf{m}}(z)$, that is $S_{\mathbf{m}}^{(-1)}\big(S_{\mathbf{m}}(z)\big) = S_{\mathbf{m}}\big(S_{\mathbf{m}}^{(-1)}(z)\big) = z$.

Let

$$R_{\mathbf{m}}(z) = \frac{1}{S_{\mathbf{m}}^{(-1)}(z)} - \frac{1}{z} \tag{3.4}$$

be the *Voiculescu R–transform* of measure $\mathbf{m}$.

Define the function $\mathrm{H}_{\mathbf{m}}(u)$ as

$$\mathrm{H}_{\mathbf{m}}(u) = \int_0^{\ln(u)} R_{\mathbf{m}}(t)dt + \ln\left(\frac{\ln(u)}{u-1}\right), \tag{3.5}$$

which should be understood as a power series in $(u-1)$.

Note that we have the following expression for its derivative:

$$\mathrm{H}'_{\mathbf{m}}(u) = \frac{1}{uS^{(-1)}_{\mathbf{m}}(\log u)} - \frac{1}{u-1}. \tag{3.6}$$

Lemma 3.3. *If* $\mathbf{m}$ *is a measure with compact support, then* $\mathrm{H}_{\mathbf{m}}(u)$ *as a power series in* $(u-1)$ *is uniformly convergent in an open neighborhood of* 1.

Proof. Immediately follows from the definitions. □

We will need the following mild technical assumption.

Definition 3.4. *A sequence of signatures* $\lambda(N) \in \mathbb{GT}_N$ *is called* regular*, if there exists a piecewise–continuous function* $f(t)$ *and a constant* C *such that*

$$\lim_{N\to\infty} \frac{1}{N} \sum_{j=1\ldots,N} \left| \frac{\lambda_j(N)}{N} - f(j/N) \right| = 0 \tag{3.7}$$

and

$$\left| \frac{\lambda_j(N)}{N} - f(j/N) \right| < C, \qquad j = 1, \ldots, N, \quad N = 1, 2, \ldots. \tag{3.8}$$

Remark 3.5. *Informally, the condition* (3.7) *means that scaled by* N *coordinates of* $\lambda(N)$ *approach a limit profile* f*. The restriction that* $f(t)$ *is piecewise–continuous is reasonable, since* $f(t)$ *is a limit of monotonous functions and, thus, is monotonous* (*therefore, we only exclude the case of countably many points of discontinuity for* f)*. We use condition* (3.8) *since it guarantees that all the measures which we assign to signatures and their limits have* (*uniformly*) *compact supports — thus, these measures are uniquely defined by their moments.*

Theorem 3.6. ([7], [19],[20]) *Suppose that* $\lambda(N) \in \mathbb{GT}_N$*,* $N = 1, 2, \ldots$ *is a regular sequence of signatures, such that*

$$\lim_{N\to\infty} m[\lambda(N)] = \mathbf{m}.$$

Then for any $j = 1, 2, \ldots, N$ *we have*

$$\lim_{N\to\infty} \frac{1}{N} \ln \left(\frac{s_{\lambda(N)}(u_1, \ldots, u_j, 1^{N-j})}{s_{\lambda(N)}(1^N)} \right) = \mathrm{H}_{\mathbf{m}}(u_1) + \cdots + \mathrm{H}_{\mathbf{m}}(u_j), \tag{3.9}$$

where the convergence is uniform over an open (*complex*) *neighborhood of* $(1, \ldots, 1)$.

The uniform measure on the set of domino tilings of a rectangular Aztec diamond $\mathcal{R}(N, \Omega, m)$ induces a measure on the set of all possible configurations of $N - \lfloor \frac{k-1}{2} \rfloor$ V-squares in the k-th row, for $k = 1, \ldots, 2N$. Due to Theorem 2.13 we can think of it from the other prospective, more precisely, as a measure on the signatures $\lambda \in \mathbb{GT}_{N-\lfloor \frac{k-1}{2} \rfloor}$. Let us denote the measure we get on the set of signatures by ρ^k and $\lfloor \frac{k-1}{2} \rfloor$ by t.

Lemma 3.7.

(3.10)

$$\begin{cases} \mathcal{S}^{U(N)}_{\rho^k}(u_1, \ldots, u_{N-t}) = \frac{s_\omega(u_1,\ldots,u_{N-t},1^t)}{s_\omega(1^N)} \prod_{j=1}^{N-t} \left(\frac{1+u_j}{2} \right)^t, & k = 2t+1, \ t = 0, 1, \ldots, N-1; \\ \mathcal{S}^{U(N)}_{\rho^k}(u_1, \ldots, u_{N-t}) = \frac{s_\omega(u_1,\ldots,u_{N-t},1^t)}{s_\omega(1^N)} \prod_{j=1}^{N-t} \left(\frac{1+u_j}{2} \right)^{t+1}, & k = 2t+2, \ t = 0, 1, \ldots, N-1. \end{cases}$$

Proof. This statement is an immediate corollary of Proposition 2.13. □

We consider $N \to \infty$ asymptotics such that all the dimensions of $\mathcal{R}(N, \Omega(N), m(N))$ linearly grow with N. Assume that the sequence of signatures $\omega(N)$ corresponding to the first row is regular and $\lim_{N\to\infty} m[\omega(N)] = \mathbf{m}_\omega$. Then from Theorem 3.6 it follows that for any $j = 1, 2, \dots, N$

$$\lim_{N\to\infty} \frac{1}{N} \ln \left(\frac{s_{\lambda(N)}(u_1, \dots, u_j, 1^{N-j})}{s_{\lambda(N)}(1^N)} \right) = \mathrm{H}_{\mathbf{m}_\omega}(u_1) + \dots + \mathrm{H}_{\mathbf{m}_\omega}(u_j). \tag{3.11}$$

Let us look at what is happening at the k-th row, we assume that $k = [2\kappa N]$. It has N minus $t = \lfloor \frac{k-1}{2} \rfloor$ V-squares. We have

$$\begin{aligned} \lim_{N\to\infty} \frac{1}{(1-\kappa)N} \log \left(\mathcal{S}^{U(N)}_{\rho^k_N}(u_1, \dots, u_j, 1^{N-t-j}) \right) = \\ = \lim_{N\to\infty} \frac{1}{(1-\kappa)N} \log \left(\frac{s_\omega(u_1, \dots, u_j, 1^{N-t-j})}{s_\omega(1^N)} \prod_{i=1}^{j} \left(\frac{1+u_i}{2} \right)^{t/t+1} \right) = \\ = \sum_{i=1}^{j} \left(\frac{\kappa}{1-\kappa} \log \left(\frac{1+u_i}{2} \right) + \frac{1}{1-\kappa} \mathrm{H}_{\mathbf{m}_\omega}(u_i) \right). \end{aligned} \tag{3.12}$$

Thus, from Theorem 3.2 we get the following proposition.

Proposition 3.8. *Assume that the sequence of signatures $\omega(N)$ corresponding to the first row is regular and $\lim_{N\to\infty} m[\omega(N)] = \mathbf{m}_\omega$. Random measures $m[\rho^k(N)]$ converge as $N \to \infty$ in probability, in the sense of moments to a* deterministic *measure $\mathbf{m}^\kappa$ on $\mathbb{R}$, whose moments are given by*

$$\int_{\mathbb{R}} x^j \mathbf{m}^\kappa(dx) = \frac{1}{2(j+1)\pi \mathbf{i}} \oint_1 \frac{dz}{z} \left(zQ'(z) + \frac{z}{z-1} \right)^{j+1}, \tag{3.13}$$

where $Q'(u) = \frac{1}{1-\kappa} \left(\frac{\kappa}{1+u} + \mathrm{H}'_{\mathbf{m}_\omega}(u) \right)$ and the integration goes over a small positively oriented contour around 1.

Proof. From Theorem 3.2 using the integral representation of the derivative we get

$$\begin{aligned} M_j(\mathbf{m}^k) &= \sum_{\ell=0}^{j} \frac{j!}{\ell!(\ell+1)!(j-\ell)!} \frac{\partial^\ell}{\partial u^\ell} \left(u^j Q'(u)^{j-l} \right) \Big|_{u=1} \\ &= \frac{1}{2\pi \mathbf{i}} \oint_1 \sum_{l=0}^{j} \frac{1}{l+1} \binom{j}{l} \frac{z^j Q'(z)^{j-l}}{(z-1)^{l+1}} dz \\ &= \frac{1}{2\pi \mathbf{i}} \oint_1 \frac{z^j Q'(z)^{j+1}}{j+1} \sum_{l=-1}^{j} \binom{j+1}{l+1} \frac{1}{Q'(z)^{l+1}(z-1)^{l+1}} dz \\ &= \frac{1}{2\pi \mathbf{i}} \oint_1 \frac{z^j Q'(z)^{j+1}}{j+1} \left(1 + \frac{1}{Q'(z)(z-1)} \right)^{j+1} dz \\ &= \frac{1}{2(j+1)\pi \mathbf{i}} \oint_1 \frac{dz}{z} \left(zQ'(z) + \frac{z}{z-1} \right)^{j+1}. \end{aligned} \tag{3.14}$$

□

Remark 3.9. *Proposition 3.8 implies the existence of a limit shape for the model we are considering. As we noted in the introduction, this result is not new, it follows from* [14], [27]. *However, Proposition 3.8 supplies explicit formulas for the answer which allows the further study of properties of limit shapes.*

In particular, we can put the computation of this limit shape into the context of the quantized free convolution. This notion (introduced in [7]*) is closely but non-trivially related to the notion of the free convolution, a well-known operation introduced by D. Voiculescu (see e.g.* [35] *). The computation of the limit shape in our case results in the folowing algorithm: we start with an arbitrary measure with compact support* $\mathbf{m}_w$*, then consider a semigroup* $\mathbf{m}_w \otimes t\mathcal{B}$*,* $t > 0$*, where* $\mathcal{B}$ *is an extreme beta character, and finally compute quantized free projections of the measures from this semigroup. We refer to* [7] *for definitions of these operations.*

The relation between tiling models and free probability is very interesting and yet to be well-understood. See Remark 6.9 for further comments.

3.2. **Height function.**

Definition 3.10. [13] *Let* $D \in \mathfrak{D}(N, \Omega, m)$ *be a domino tiling of a rectangular Aztec diamond* $\mathcal{R}(N, \Omega, m)$*. Let us impose checkboard coloring on the plane* (i, j) *such that the boundary row of* $\mathcal{R}(N, \Omega, m)$ *consists of the dark squares, see Figure 11. A height function* h_D *is an integer-valued function on the vertices of the lattice squares of* $\mathcal{R}(N, \Omega, m)$ *which satisfies the following properties:*

- *if an edge* (u, v) *does not cross any domino in* D *then* $h(v) = h(u) + 1$ *if* (u, v) *has a dark square on the left, and* $h(v) = h(u) - 1$ *otherwise.*
- *if an edge* (u, v) *crosses a domino in* D *then* $h(v) = h(u) + 3$ *if* (u, v) *has the dark square on the left, and* $h(v) = h(u) - 3$ *otherwise.*
- $h_D(u_0) = 0$*, where* u_0 *is the vertex in the upper right corner of* $\mathcal{R}(N, \Omega, m)$*, see Figure 11.*

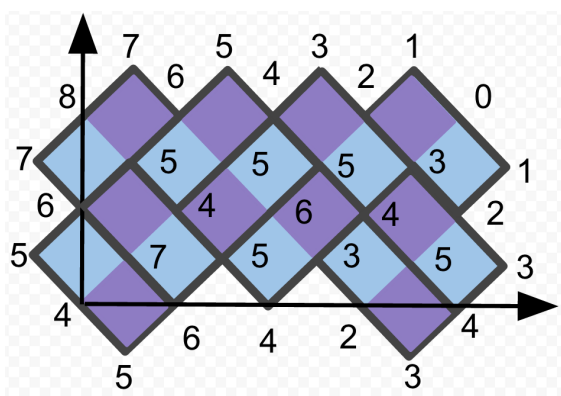

FIGURE 11. An example of a domino tiling of $\mathcal{R}(2, \Omega = (1, 4), 2)$ and its height function.

Fix a domino tiling $D \in \mathfrak{D}(N, \Omega, m)$. Note that the height function is uniquely determined on the boundary of the domain. Let us calculate it inside. Consider a vertex (i, j) inside the domain. It is the left-most vertex of a unit square that belongs to a row with number $(2j+1)$. Such a row contains $(N - \lfloor j \rfloor)$ V-squares. Let $Y_{\mu^{D,j}}$ be the Young diagram corresponding to

this row under the Construction 2.7, where $\mu^{D,j} = (\mu_1^{D,j} \geqslant \mu_2^{D,j} \geqslant \cdots \geqslant \mu_{N-\lfloor j \rfloor}^{D,j})$. Define the function

$$\Delta_D^N(i,j) := \left|\left\{1 \leqslant s \leqslant N - \lfloor j \rfloor : \mu_s^{D,j} + (N - \lfloor j \rfloor) - s \geqslant i\right\}\right|. \tag{3.15}$$

Denote by p_k the position of the k-th V-square in this row counting from the left. By construction we have

$$\mu_s^{D,j} + (N - \lfloor j \rfloor) - s = p_{N-\lfloor j \rfloor - s+1} - 1.$$

Thus, $\Delta_D^N(i,j)$ simply counts the number of V-squares to the right from the vertex (i,j) in the corresponding row. Note that we can rewrite it in terms of the measure $m[\mu^{D,j}]$

$$\Delta_D^N(i,j) = (N - \lfloor j \rfloor) \int 1_{[\frac{i}{N-\lfloor j \rfloor}, \infty]} dm[\mu^{D,j}]. \tag{3.16}$$

Lemma 3.11. *Let $D \in \mathfrak{D}(N, \Omega, m)$ be a domino tiling of the rectangular Aztec diamond $\mathcal{R}(N, \Omega, m)$. Let (i,j) be a vertex inside the domain. Then*

$$h_D((i,j)) = 2\left(2N + m - j - \lfloor i \rfloor - 2\Delta_D^N(i,j)\right), \ j = 0, \ldots, N. \tag{3.17}$$

Proof. Consider a path from $(-\frac{1}{2}, j)$ to $(N + m + \frac{1}{2}, j)$ for the even rows and a path from $(0, j)$ to $(N + m, j)$ for the odd rows constructed in the following way. It is allowed to go from vertex (i,j) to $(i+1,j)$ along the boundary of a domino $d \in D$, see Figure 12.

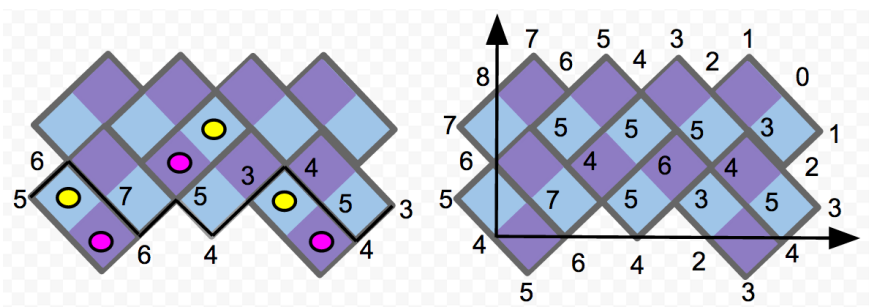

FIGURE 12. An example of a domino tiling of $\mathcal{R}(2, \Omega = (1,4), 2)$ and its height function.

By the definition of the height function with every step along this path it changes by two. The sign of this change depends on whether the path goes along the boundary of a V-square or a Λ-square. Let us follow this path from right to left. Then the height function increases by two if the path goes along the boundary of a Λ-square and decreases by two otherwise. Note that the number of squares to the right from the vertex (i,j) is equal to $(N + m - \lfloor i \rfloor)$. So the total increment of the height function is equal to

$$2\left(\#\{\Lambda - \text{squares}\} - \#\{V - \text{squares}\}\right) = 2\left((N + m - \lfloor i \rfloor) - 2\#\{V - \text{squares}\}\right).$$

Thus, what is left is to compute the value of the height function on the right boundary of the domain. It is easily done by going alone the boundary starting from the point u_0. We see that it is equal to $2(N - j)$. $\square$

Theorem 3.12. (*Law of Large numbers for the height function.*) *Consider $N \to \infty$ asymptotics such that all the dimensions of a rectangular Aztec diamond $\mathcal{R}(N, \Omega(N), m(N))$ linearly grow with N. Assume that the sequence of signatures $\omega(N)$ corresponding to the first row is regular and $\lim\limits_{N\to\infty} m[\omega(N)] = \mathbf{m}_\omega$. Let us fix $\kappa \in (0,1)$ and let $\mathbf{m}^\kappa$ be the limit of measures $m[\rho_k(N)]$, which exists due to Proposition 3.8.*

Define

$$\mathbf{h}(\chi,\kappa) := 2\left(2+\nu-\kappa-\chi-2(1-\kappa)\int\limits_{\frac{\chi}{1-\kappa}}^{\infty} \mathbf{dm}^\kappa(x)\right).$$

Then random height function $h_{\mathfrak{D}}$ obeys the following law of large numbers with almost sure convergence

$$\frac{h_{\mathfrak{D}}([\chi N],[\kappa N])}{N} \to \mathbf{h}(\chi,\kappa), \text{ as } N\to\infty,$$

where (χ,κ) are the new continuous parameters of the domain and $\frac{m(N)}{N} \to \nu$ as N goes to infinity.

Proof. From Lemma 3.11 we see that for a fixed $j = [\kappa N]$ the height function is the scaled distribution function of the measure $m[\rho^k]$, where k is the number of the corresponding row. Thus, from Proposition 3.8 the Law of Large numbers follows.

□

4. Characterization of the support of the limit measure

In what follows we consider $N \to \infty$ asymptotics such that all the dimensions of a rectangular Aztec diamond $\mathcal{R}(N, \Omega(N), m(N))$ linearly grow with N. The limit domain scaled by N is denoted $\mathcal{R}$ and the new continuous coordinates inside the domain are (χ,κ). We also assume that the sequence of signatures $\omega(N)$ corresponding to the first row is regular and the sequence of measures $\{m[\omega(N)]\}$ weakly converge to $\mathbf{m}_\omega$. In this section our goal is to compute the density of the limit measures $\mathbf{m}^\kappa$.

4.1. Preliminaries.

Note that under our assumptions $\mathbf{m}_\omega$ has compact support. Moreover, it is continuous with respect to Lebesgue measure and its density takes values in $[0,1]$.

Recall that a Stieltjes transform of a compactly-supported measure m is defined as

$$\mathrm{St}_m(t) = \int\limits_{\mathbb{R}} \frac{m[ds]}{t-s},$$

for $t \in \mathbb{C}\backslash\mathrm{Support}(\mathbf{m})$.

Let $x \in \mathbb{C}$ and $\kappa \in (0,1)$. Consider the following system of equations in z and t, where $z \in \mathbb{C}\backslash\mathbb{R}_-$ and $t \in \mathbb{C}\backslash\mathrm{Support}(\mathbf{m}_\omega)$

$$\begin{aligned} \mathbf{F}_\kappa(z,t) &= x, \\ \mathrm{St}_{\mathbf{m}_\omega}(t) &= \log(z), \end{aligned} \tag{4.1}$$

where we consider the principal branch of the logarithm and

$$\mathbf{F}_\kappa(z,t) = \frac{z}{(1-\kappa)}\Big(\frac{t}{z} - \frac{1}{(z-1)} + \frac{\kappa}{1+z}\Big) + \frac{z}{z-1}. \tag{4.2}$$

Note that if (z_0, t_0) is the solution to (4.1), then applying the complex conjugation we obtain another solution $(\bar{z}_0, \bar{t}_0)$.

Proposition 4.1. *The system of equations (4.1) for $x \in \mathbb{R}$ has at most a pair of solutions (z_0, t_0) and $(\bar{z}_0, \bar{t}_0)$, where z_0 is not a real number.*

Proof. We will first prove this statement for a special case of measure $\mathbf{m}_\omega$. Let us fix a natural number s and let $(a_1, a_2, \dots, a_s)$ and $(b_1, b_2, \dots, b_s)$ be two s-tuples of real numbers such that

$$a_1 < b_1 < a_2 < b_2 \cdots < a_s < b_s \text{ and } \sum_{i=1}^{s}(b_i - a_i) = 1.$$

Assume that $\mathbf{m}_\omega$ is a uniform measure on the union of the intervals $[a_i, b_i]$.

Then we can compute

$$\mathrm{St}_{\mathbf{m}_\omega}(t) = \log \frac{(t-a_1)\cdots(t-a_s)}{(t-b_1)\cdots(t-b_s)}.$$

Let us express t as a function of x, κ and z from the first equation of (4.1)

$$t(z,\kappa,x) = x(1-\kappa) + \frac{2\kappa z}{z^2-1} \tag{4.3}$$

and substitute it into the second one. We claim that the resulting equation (4.4) will have at most one pair of complex conjugate solutions.

Denote

(4.4)

$$\begin{aligned} P_{x,\kappa}(z) = {} & (2\kappa z + x(1-\kappa)(z^2-1) - a_1(z^2-1))\cdots(2\kappa z + x(1-\kappa)(z^2-1) - a_s(z^2-1)) - \\ & - z(2\kappa z + x(1-\kappa)(z^2-1) - b_1(z^2-1))\cdots(2\kappa z + x(1-\kappa)(z^2-1) - b_s(z^2-1)). \end{aligned}$$

Then the statement that we are aiming to prove follows from the following more general lemma. It will also be important in our further considerations.

Lemma 4.2. *Let $x \in \mathbb{R}$, $\kappa \in (0,1)$. There exist continuous real-valued functions $r_i(x)$ for $i = 1, \dots, 2s-1$ defined on $\mathbb{R}\backslash x_i$ such that $P_{x,\kappa}(r_i(x)) = 0$ and $\{x_i\}$ is some collection of points in $\mathbb{R}$. Moreover, $r_i(x)$ is a simple root of the polynomial $P_{x,\kappa}$ for any $x \in \mathbb{R}\backslash x_i$.*

Proof. Let us rewrite the equation

$$P_{x,\kappa}(z) = 0$$

in the following form

$$\begin{aligned} & (2\kappa z + x(1-\kappa)(z^2-1) - a_1(z^2-1))\cdots(2\kappa z + x(1-\kappa)(z^2-1) - a_s(z^2-1)) \\ & = z(2\kappa z + x(1-\kappa)(z^2-1) - b_1(z^2-1))\cdots(2\kappa z + x(1-\kappa)(z^2-1) - b_s(z^2-1)). \end{aligned} \tag{4.5}$$

Denote the LHS by $P_a(z)$ and the RHS by $P_b(z)$. Denote the roots of $t(x,\kappa,z) = a_s$ by $\alpha^s_\pm$ and the roots of $t(x,\kappa,z) = b_s$ by $\beta^s_\pm$.

Fix x such that $x(1-\kappa) \gg b_s > 0$. Let us look at the possible configuration of $\alpha^i_\pm$ and $\beta^i_\pm$ on the real line.

Figure 13 presents an example of a graph of the function $y = \frac{2\kappa z}{z^2-1}$. Its asymptote is $y = 0$. To obtain the graph of $t(x, \kappa, z)$ we need to lift it by $x(1-k)$.

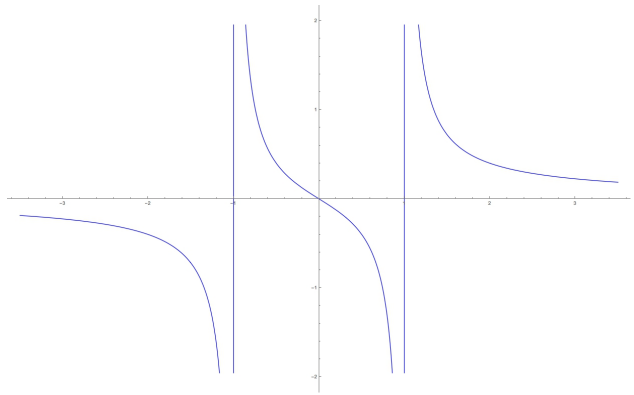

FIGURE 13. The graph of $y = \frac{2\kappa z}{z^2-1}$.

To find the roots of $P_a(z)$ and $P_b(z)$ we need to look at the intersections of the lines $y = a_i$ and $y = b_i$ and the graph of $t(x, \kappa, z)$. Due to our assumption on x all the intersections will happen below the asymptote $y = x(1-k)$. It is easy to see that we will obtain the following configuration:

$$\{\beta_-^s < \alpha_-^s < \cdots < \beta_-^1 < \alpha_-^1 < 0 < \beta_+^s < \alpha_-^s < \cdots < \beta_-^1 < \alpha_+^1\}.$$

Thus, since $\alpha_\pm^i$ and $\beta_\pm^i$ interlace there exists a simple root of $P_{x,\kappa}$ on every interval $(\alpha_\pm^i, \alpha_\pm^{i-1})$. Note that both leading coefficients of $P_a(z)$ and $P_b(z)$ are equal to $(x - \kappa x)^s > 0$ but the degree of $P_b(z)$ is $2s+1$ and the degree of $P_a(z)$ is $2s$. Therefore, there also exists a simple real root on the interval (α_-^s, α_+^1): $= (-\infty, \alpha_-^s) \cup (\alpha_+^1, \infty)$. In total we get $2s-1$ simple real roots which lie on non-intersecting intervals. Let us look at the root which lies on the interval (α_-^s, α_+^1) and the root which lies on $(\alpha_+^s, \alpha_+^{s-1})$, denote it by $r_-(x)$ and $r_+(x)$ respectively. Now our goal is to continuosly define these functions for any $x \neq \frac{a_s}{1-\kappa}$.

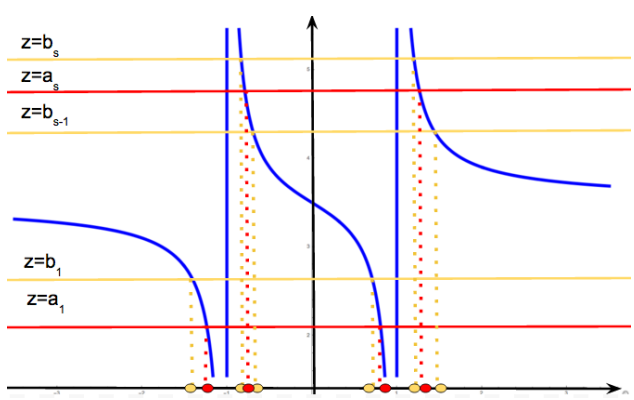

FIGURE 14. The graph of $t(\kappa, x, z)$ and the horizontal sections.

Looking at Figure 14 we notice that as $x \to \infty$ the configuration does not change and we can continue our function. When $x \to \frac{b_s}{1-\kappa}$ the point β_-^s runs to $-\infty$ and β_+^s approaches 0. Thus, the configuration changes (at this point the degree of $P_b(z)$ dropped to $2s$.)

$$\{\alpha_-^s < \cdots < \beta_-^1 < \alpha_-^1 < 0 = \beta_+^s < \alpha_+^s < \cdots < \beta_+^1 < \alpha_+^1\}$$

Nevertheless, this does not affect our function $r_\pm(x)$. Let us look at what happens when $x \to \frac{a_s}{1-\kappa}$. We see that α_-^s approaches $-\infty$ as well as $r_-(x)$, α_+^s approaches zero as well as $r_+(x)$. We will get a new configuration of points

$$\{\beta_-^{s-1} < \alpha_-^{s-1} < \cdots < \beta_-^1 < \alpha_-^1 < \beta_-^s < 0 = \alpha_+^s < \beta_+^{s-1} < \alpha_+^{s-1} < \cdots < \beta_+^1 < \alpha_+^1 < \beta_+^s < \alpha_+^s\}.$$

Next, we see that the root $r_+(x)$ passes the point α_+^s at zero and now lies on interval (α_-^1, α_-^s) (when α_+^s passes zero it becomes α_-^s). Note that it is now the unique root on this interval and we see that we can continue our function when we pass zero.

The root $r_-(x)$ passed the infinity and lies on (α_+^s, ∞). If we look at the roots which lie on the other intervals they just stay on that interval that is moving towards $-\infty$. Therefore, we conclude that the whole configuration of $\alpha_\pm^i$ and $\beta_\pm^i$ moves cyclically around infinity. To sum up, the function $r_+(x)$ has a unique point of discontinuity when $x \to \frac{a_s}{1-\kappa}$. The same strategy would work if one starts with a root which lies on a different interval. □

Note that the degree of $P_{x,\kappa}(z)$ is at most $(2s+1)$ and we have found $(2s-1)$ real roots in Lemma 4.2, therefore, we conclude that the system (4.1) has at most one pair of complex conjugate solutions, which completes the proof of the Proposition 4.1 for the special class of the measures considered.

Now let us look at a general case of measure $\mathbf{m}_\omega$. There exists a sequence of measures $\{\mu_n\}$ that converges weekly to $\mathbf{m}_\omega$, where μ_i is a uniform measure with density one on a sequence of intervals. Denote

$$p_n(z) = \mathrm{St}_{\mu_n}(t(x,\kappa,z)) - \log(z) \text{ and } p(z) = \mathrm{St}(t(x,\kappa,z)) - \log(z).$$

Both p_n and p are defined on $\mathbb{C}\backslash\mathbb{R}$. We will use an argument from part (b) of Lemma 3.1 in [15].

Lemma 4.3. *Let z_0 be a root of $p(z)$ of multiplicity $k \geqslant 1$, and choose $\epsilon > 0$ such that a ball $B(z_0, 2\epsilon)$ is in the domain of the definition of $p(z)$ and z_0 is the unique root of f in $B(z_0, 2\epsilon)$ (this is always possible since the roots of an analytic function are isolated.) Then, for all n sufficiently large, $f_n(z)$ has k roots in $B(z_0, 2\epsilon)$ counting multiplicities.*

Proof. This will follow from Rouché theorem if we can show that $|p(z)| > |p(z) - p_n(z)|$ for all n sufficiently large and $z \in \partial B(z_0, 2\epsilon)$, the boundary of $B(z_0, 2\epsilon)$. Thus, we need the following two statements. First,

$$\inf_{z\in\partial B(z_0,2,\epsilon)} |p(z)| > 0$$

since $p(z)$ is analytic in B. Second,

$$\lim_{n\to\infty} \sup_{z\in\bar{B}(z_0,2\epsilon)} |p(z) - p_n(z)| = 0,$$

which follows from the week convergence. □

Therefore, $p(z)$ can not have more than one complex root in the upper half-plane. Thus, the statement of the Proposition 4.1 follows. □

4.2. **The density of $\mathbf{m}^\kappa$.** Let us look at the system of equations (4.1) from another perspective. Recall that whenever a formal power series of the form

$$g(u) = \sum_{i=1}^{\infty} g_i u^i \in \mathbb{R}[[u]]$$

has $g_1 \neq 0$, there exists a formal power series

$$h(u) = \sum_{i=1}^{\infty} h_i u^i \in \mathbb{R}[[u]]$$

that is a composition inverse of $g(u)$, meaning that $g(h(u)) = u$.

In the case of Laurent series of the form

$$p(u) = \frac{1}{u} + \sum_{i=0}^{\infty} p_i u^i \in \mathbb{R}((u))$$

there also exists a composite inverse Laurent series $q(u) = \sum_{i=1}^{\infty} q_i (\frac{1}{u})^i \in \mathbb{R}((u))$ such that $p(q(u)) = u$.

Fix $\kappa \in (0,1)$. Note that $\mathrm{St}_{\mathbf{m}_\omega}(t)$ is a uniformly convergent power series in $\frac{1}{t}$ for t in the neighborhood of infinity.

Let

$$t(z) \colon = \mathrm{St}^{(-1)}_{\mathbf{m}_\omega}(\log z),$$

which we view as a Laurent series in $(z-1)$. More precisely, we have

$$\mathrm{St}^{(-1)}_{\mathbf{m}_\omega}(\log z) = \frac{1}{z-1} + \sum_{i=0}^{\infty} u_i (z-1)^i.$$

Substituting this formula into $F_\kappa(z,t)$ (4.1) we obtain the following expression for $F_\kappa(z)$ as Laurent series in $(z-1)$:

$$F_\kappa(z) = \frac{1}{z-1} + \sum_{i=0}^{\infty} f_i (z-1)^i.$$

This series is uniformly convergent for z in the punctured neighborhood of 1.

Define $z^\kappa(x)$ as the composite inverse to $F_\kappa(z)$. Note that $z^\kappa(x)$ is formal power series in $\frac{1}{x}$, which is uniformly convergent for x in the neighborhood of infinity.

Lemma 4.4. *The following formula is valid for x in the neighborhood of infinity*

$$\mathrm{St}_{\mathbf{m}^\kappa}(x) = -\log(z^\kappa(x)),$$

where $\mathrm{St}_{\mathbf{m}^\kappa}(x)$ is the Stieltjes transform of the limit measure $\mathbf{m}^\kappa$.

Proof. We know from Proposition 3.8 that the j-th moment of measure $\mathbf{m}^\kappa$ can be computed as

$$M_j(\mathbf{m}^\kappa) = \frac{1}{2(j+1)\pi \mathbf{i}} \oint_1 \frac{dz}{z} \left(\frac{z}{(1-\kappa)} \left(\mathrm{H}'_{\mathbf{m}_\omega}(z) + \frac{\kappa}{1+z} \right) + \frac{z}{z-1} \right)^{j+1},$$

where the contour of integration is a circle of radius $\epsilon \ll 1$ around 1.

Using the formula (3.6) for $\mathrm{H}'_{\mathbf{m}}$ we get

$$\frac{z}{(1-\kappa)}\left(\mathrm{H}'_{\mathbf{m}_\omega}(z)+\frac{\kappa}{1+z}\right)+\frac{z}{z-1}=F_\kappa(z).$$

Now we can compute the Stieltjes transform for x in the neighborhood of infinity as

$$\sum_{j=0}^{\infty}\frac{M_j(\mathbf{m}^\kappa)}{x^{j+1}}=-\frac{1}{2\pi\mathbf{i}}\oint_1\frac{dz}{z}\log\left(1-\frac{\mathbf{F}_\kappa(z)}{x}\right).$$

Integrating by parts we get

$$\sum_{j=0}^{\infty}\frac{M_j(\mathbf{m}^\kappa)}{x^{j+1}}=-\frac{1}{2\pi\mathbf{i}}\oint_1\log(z)\frac{\partial_z\left(1-\frac{\mathbf{F}_\kappa(z)}{t}\right)}{1-\frac{\mathbf{F}_\kappa(z)}{x}}.$$

For x large enough the integral has a unique pole at $1-\frac{\mathbf{F}_\kappa(z)}{x}=0$ and it is given by the unique composite inverse of the Laurent series $\mathbf{F}_\kappa(z)$ for z in the neighborhood of 1. We need to compute the residue to obtain the final result. Thus, we get

$$\mathrm{St}_{\mathbf{m}^\kappa}(x)=-\log(z^\kappa(x))$$

for x in a neighborhood of infinity. □

Let us define a function

$$\mathbf{Z}^\kappa(x)=\exp(-\mathrm{St}_{\mathbf{m}^\kappa}(x)),$$

where $x\in\mathbb{C}\backslash\mathrm{Support}(\mathbf{m}^\kappa)$.

Note that due to Lemma 4.4

$$F_\kappa(\mathbf{Z}^\kappa(x))=0 \tag{4.6}$$

for x in the neighborhood of infinity. Since the left-hand side of this equation is an analytic function on its domain of definition, the equality holds for any $x\in\mathbb{C}\backslash\mathrm{Support}(\mathbf{m}^\kappa)$. Therefore, $\mathbf{Z}^\kappa(x)$ is one of the roots of (4.1).

Let us recall a well-known fact about Stieltjes transform of a measure, see [1].

Lemma 4.5. *If a measure μ has a continuous density $f(x)$ with respect to the Lebesgue measure then the following formula is valid*

$$f(x)=-\lim_{\epsilon\to0^+}\frac{1}{\pi}\mathrm{Im}(\mathrm{St}_\mu(x+i\epsilon)).$$

We know that according to Lemma 4.1 the system of equations (4.1) has at most one root in the upper half-plane $\mathbb{H}:=\{z\in\mathbb{C}:\mathfrak{I}(z)>0\}$ for $x\in\mathbb{R}$. Thus, from Lemma 4.5 and from (4.6) we get that if the density $\mathbf{dm}^\kappa$ is non-zero at a point x_0 it has to be equal to $\frac{1}{\pi}\mathrm{Arg}$(unique complex root in $\mathbb{H}$ of (4.1) when $x=x_0$). Note that measure $\mathbf{m}^\kappa$ has a non-empty support because its Stieltjes transform is not identically zero.

Proposition 4.6. *The density of $\mathbf{m}^\kappa$ can be computed in the following way*

$$\mathbf{dm}^\kappa(x)=\frac{1}{\pi}\mathrm{Arg}(\mathbf{z}^\kappa_+(x)), \tag{4.7}$$

where $\mathbf{z}^\kappa_+(x)$ is the unique complex root of the system (4.1) which belongs to the upper half-plane. This formula is valid for such (x,κ) that the complex root exists, the density is equal to zero or one otherwise.

Proof. Let $\mathbf{m}_\omega$ be a uniform meaure of density 1 on the finite union of intervals $\cup_{i=1}^s [a_i, b_i]$. Then

$$P_{x,\kappa}(\mathbf{Z}^\kappa(x)) = 0,$$

where $P_{x,\kappa}(z)$ is defined by (4.4). Due to Lemma 4.2 we know that for any $x \in \mathbb{R}$ the polynom $P_{x,\kappa}(z)$ has $(2s-1)$ simple roots $r_i(x)$. From the Implicit function theorem follows that $r_i(x)$ are analytic functions defined on some neighborhood of the punctured real line. Therefore, if $\mathbf{Z}^\kappa(x)$ coincides with $r_i(x)$ at a point x_0 for some i, then $\mathbf{Z}^\kappa(x)$ coincides with $r_i(x)$ on the whole domain of the definition of the latter function. Also, we know that the domain of discontinuity of $\mathbf{Z}^\kappa(x)$ on $\mathbb{R}$ is presicely Support$(\mathbf{m}^\kappa)$, therefore, it cannot coincide with any $r_i(x)$, unless, the support is just one point. We conclude that whenever $x \in \mathbb{R}$ is such that $P_{x,\kappa}$ has a pair of complex conjugate roots $(z_-^\kappa(x), z_+^\kappa(x))$ (recall that this pair is always unique) $\mathbf{Z}^\kappa(x)$ is equal to $z_-^\kappa(x)$. This conlcudes the proof of Proposition 4.6 for this class of measures.

Now let us consider a general case of measure $\mathbf{m}_\omega$. There exists a sequence of measures $\{\mu_n\}$ that converges weekly to $\mathbf{m}_\omega$, where μ_i is a uniform measure with density one on a sequence of intervals. Then we can pass to the limit in the equation (4.7). □

Remark 4.7. *Note that the scaling which we use computing* $\mathbf{m}^\kappa$ *is* $\frac{1}{(1-\kappa)N}$, *however, the coordinates of the domain scale as* $\frac{1}{N}$.

Definition 4.8. *Let* $\mathcal{L}$ *be the set of* (χ, κ) *inside* $\mathcal{R}$ *such that the density* $\mathbf{dm}^\kappa(\frac{\chi}{1-\kappa})$ *is not equal to* 0 *or* 1. *Then* $\mathcal{L}$ *is called the liquid region. Its boundary* $\partial\mathcal{L}$ *is called the frozen boundary.*

Note that the density $\mathbf{dm}^\kappa(\frac{\chi}{1-\kappa})$ is not equal to 0 or 1 if and only if the system (4.1) has a complex solution for $(\chi, \kappa) \in \mathcal{R}$.

5. Frozen boundary

We will consider a special case of a rectangular Aztec diamond $\mathcal{R}(N, \Omega, m)$ with

$$\Omega = (A_1, \dots, B_1, A_2, \dots, B_2, \dots, A_s, \dots, B_s), \text{ where } \sum_{i=1}^s (B_i - A_i + 1) = N,$$

see Figure 15.

Denote the string $(A_1, A_2 \dots, A_s)$ by $A^{(s)}$ and the string $(B_1, B_2 \dots, B_s)$ by $B^{(s)}$. We call such domain a *rectangular Aztec diamond of type* $(N, A^{(s)}, B^{(s)})$.

We are interested in the following asymptotic regime of its growth :

$$A_i(N) = [a_i N],\ m(N) = [\mu N],\ B_i(N) = [b_i N],$$

where $a_1 < b_1 < \dots < a_s < b_s$ are new parameters such that $\sum_{i=1}^s (b_i - a_i) = 1$. We will call s the number of segments.

The sequence of signatures $\{\omega(N)\}$ is regular and the limit measure $\mathbf{m}_\omega$ is a uniform measure on the union of intervals $[a_i, b_i]$ considered in the proof of the Proposition 4.1.

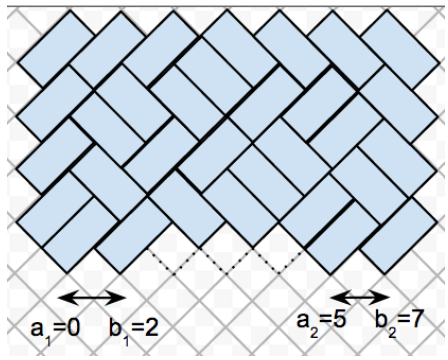

FIGURE 15. Rectangular Aztec diamond $\mathcal{R}(4,(1,2,6,7),3)$ with $A_1=1$, $B_1=2$, $A_2=6$, $B_2=7$.

Theorem 5.1. *The frozen boundary of the limit of a rectangular Aztec diamond of type* $(N, A^{(s)}, B^{(s)})$ *is a rational algebraic curve* C *with an explicit parametrization* (5.2)*. Moreover, its dual* $C^\vee$ *is of degree* $2s$ *and is given in the following parametric form*

$$C^\vee = \left(\theta,\ \frac{2\theta\Pi_s(t)}{(\Pi_s(\theta)-1)(\Pi_s(\theta)+1)}\right), \tag{5.1}$$

where

$$\Pi_s(\theta) = \frac{(1-a_1)(1-a_2\theta)\cdots(1-a_s\theta)}{(1-b_1\theta)(1-b_2\theta)\cdots(1-b_s\theta)}.$$

Proof. From Lemma 4.2 it follows that the frozen boundary is given by the discriminant of $P_{\frac{\chi}{1-\kappa},\kappa}(z)$. More precisely, it is the set of points (χ,κ), where $P_{\frac{\chi}{1-\kappa},\kappa}(z)$ has a double root.

In the case of a rectangular Aztec diamond of type $(N, A^{(s)}, B^{(s)})$ we can rewrite the system of equations (4.1) in the following form:

$$\begin{cases} \frac{(t-a_1)(t-a_2)\cdots(t-a_s)}{(t-b_1)(t-b_2)\cdots(t-b_s)} = z, \\ F_\kappa(z) = \frac{z}{(1-\kappa)}\left(\frac{t}{z} - \frac{1}{z-1} + \frac{\kappa}{1+z}\right) + \frac{z}{z-1} = \frac{\chi}{(1-\kappa)}, \end{cases}$$

Let us express z from the second equation and plug it into the first one. We find that

$$z^{\pm}(t,\kappa) = \frac{\kappa \pm \sqrt{\kappa^2+(t-\chi)^2}}{t-\chi}.$$

Let us introduce the following notation $\mathrm{L}\Pi_s(t) = \log \Pi_s(t)$.

The condition that the resulting equation has a double root can be rewritten as the following system

$$\begin{cases} \Pi_s(t) = z^{\pm}(t,\kappa), \\ \mathrm{L}\Pi_s(t)' = (\log(z^{\pm}(t,\kappa))))'. \end{cases}$$

This system can be solved for χ and κ and we find that

$$\chi(t) = \frac{\Pi_s(t)^2\mathrm{L}\Pi_s(t)t + \mathrm{L}\Pi_s(t)t + \Pi_s(t)^2 - 1}{(\Pi_s(t)^2+1)\mathrm{L}\Pi_s(t)} \text{ and } \kappa(t) = -\frac{(\Pi_s(\theta)^2-1)^2}{2(\Pi_s(t)^2+1)\Pi_s(t)\mathrm{L}\Pi_s(t)}. \tag{5.2}$$

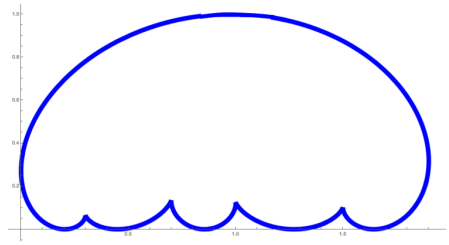

FIGURE 16. An example of a curve C with three boundary segments.

This gives us the parametric representation of the frozen boundary. In order to compute its dual we use the standard formulas:

$$x^\vee = \frac{y'}{yx' - xy'};$$
$$y^\vee = -\frac{x'}{yx' - xy'}.$$

Note that $\Pi_s(t)' = \Pi_s \cdot \mathrm{L}\Pi_s(t)$. Using this relation we get the parametric representation (5.1) of the dual curve after some lengthy computation, where we introduced the parameter $\theta = \frac{1}{t}$.

From the parametric representation it is easy to see that the degree of the dual curve is equal to $2s$.

□

Definition 5.2. [27] *A degree d real algebraic curve $C \subset \mathbb{R}\mathrm{P}^2$ is winding if*

- *It intersects every line $L \subset \mathbb{R}\mathrm{P}^2$ in at least $d-2$ points counting multiplicity;*
- *There exists a point $p_0 \in \mathbb{R}\mathrm{P}^2 \backslash C$ called center, such that every line through p_0 intersects C in d points.*

The dual to a winding curve is called a cloud curve.

Proposition 5.3. *The frozen boundary C is a cloud curve of rank $2s$, where s is the number of segments. Moreover, it is tangent to the following $4s$ lines counting multiplicity*

$$\mathcal{L} = \{\chi = a_i | i = 1, \dots, s\} \cup \{\chi = b_i | i = 1, \dots, s\} \cup \{\kappa = 0\} \cup \{\kappa = 1\}.$$

Proof. We need to check that the dual curve $C^\vee = (x, y)$ is winding. Let us write down the equation for the dual curve in terms of x and y. Let us denote

$$P_a(x) = (1 - a_1 x)(1 - a_2 x) \dots (1 - a_s x) \text{ and } P_b(x) = (1 - b_1 x)(1 - b_2 x) \dots (1 - b_s x).$$

In terms of x and y we get the following equation of $C^\vee$

$$y(P_a(x) - P_b(x))(P_a(x) + P_b(x)) - 2xP_a(x)P_b(x) = 0 \tag{5.3}$$

Note that $P_a(0) = P_b(0) = 1$. Thus, the rank of C is $2s$.

We need to compute the intersection of $C^\vee$ with any given line in $\mathbb{R}\mathrm{P}^2$. Let us start with the lines given by $y = cx + d$, where $c, d \in \mathbb{R}$. Then the points of intersection satisfy the following equation

$$(cx + d)(P_a(x) - P_b(x))(P_a(x) + P_b(x)) = 2xP_a(x)P_b(x). \tag{5.4}$$

We will use the same strategy as in Lemma 4.1. We can assume that $a_1 > 0$ since we can move the limit rectangle to the right along the χ axis, which does not effect the geometric properties of the frozen boundary. The roots of the RHS of equation (5.4) are $\{0, \frac{1}{a_1}, \frac{1}{b_1}, \dots, \frac{1}{a_s}, \dots, \frac{1}{b_s}\}$. Since $\{a_i\}$ and $\{b_i\}$ interlace, all the roots of $p_- = P_a(x) - P_b(x)$ and $p_+ = P_a(x) + P_b(x)$ are real and there are $2s-1$ distinct roots. Moreover, there exist two roots of $p_\pm$ in every interval $(\frac{1}{a_{i+1}}, \frac{1}{a_i})$ and the point $\frac{1}{b_i}$ lies in between those roots. Therefore, the roots of the polynomial given by the LHS of (5.4) interlace with the roots of the polynomial given by the RHS with probably an exception of an interval containing the zero of $cx+d$. So we have found at least $2s-2$ real points of intersection of our curve with lines of the form $y = cx+d$.

Next, consider the lines $x = d$. The intersection will be at infinity. We need to consider the homogenized polynomial that defines our curve adding the third homogeneous coordinate z.

$$y(P_a(x,z) - P_b(x,z))(P_a(x,z) + P_b(x,z)) - 2xP_a(x,z)P_b(x,z) = 0,$$

$$P_a(x,z) = (z - a_1x)(z - a_2x)\dots(z - a_sx) \text{ and } P_b(x,z) = (z - b_1x)(z - b_2x)\dots(z - b_sx).$$

The homogenious form of the equation of the line is $x = dz$. Thus, we see that this line intersects the curve at the point $(0:1:0)$ with multiplicity $2s-1$. The case of the line $z = 0$ is analogous.

Note that due to the computation above if we choose a point p_0 on the line $y = 0$ outside the interval $(0, \frac{1}{a_1})$ any line passing through p_0 will intersect the curve $C^\vee$ at at least $2s-1$ real points. Therefore, any line through p_0 will intersect $C^\vee$ at exactly $2s$ real points. So the point p_0 can be chosen to be the center.

Notice that the points $(x,y) = (0, \frac{1}{a_i})$ as well as $(x,y) = (0, \frac{1}{b_i})$ belong to $C^\vee$. The roots of $(P_a(x) - P_b(x))(P_a(x) + P_b(x))$ correspond to $2s-1$ points of tangency of C with the line $\kappa = 0$. Also, when $x = 0$ the y coordinate of $C^\vee$ is 1, which corresponds to the tangent $\kappa = 1$ of C. From these the second statement of the proposition follows.

□

Remark 5.4. *From* (5.1) *and* (5.2) *we see that the points of tangency of* $C = (\chi(\theta), \kappa(\theta))$ *with* $\kappa = 0$, *that is, with the side of rectangle with non-trivial boundary conditions, are precisely the roots of*

$$\prod_{i=1}^{s} \frac{x - a_i}{x - b_i} = \pm 1.$$

6. Gaussian Free Field

6.1. **Characterization of the liquid region.** By Proposition 4.6 $(\chi, \kappa) \in \mathcal{L}$ if and only if the system of equations (4.1) has complex roots. Let us recall it

$$\begin{cases} \mathbf{F}_\kappa(z,t) = \frac{\chi}{(1-\kappa)}, \\ \mathrm{St}_{\mathbf{m}_\omega}(t) = \log(z), \end{cases}$$

where

$$\mathbf{F}_\kappa(z,t) = \frac{z}{(1-\kappa)}\Big(\frac{t}{z} - \frac{1}{(z-1)} + \frac{\kappa}{1+z}\Big) + \frac{z}{z-1}.$$

From the first equation we find that

$$z_{\pm}(\chi,\kappa)(t) = \frac{\kappa \pm \sqrt{\kappa^2 + (t-\chi)^2}}{t-\chi}. \tag{6.1}$$

and

$$t = \frac{\chi z^2 + 2\kappa z - \chi}{z^2 - 1}. \tag{6.2}$$

It follows that $z_{\pm}(\chi,\kappa)$ is complex if and only if t is (if one of them is real then the other one has to be real too).

Recall that $\mathbb{H}$ is the upper halfplane of the complex plane.

Lemma 6.1. *Let $t \in \mathbb{H}$. Then there exists $z(t)$ such that $(z(t),t)$ is the solution to (4.1) if and only if the following equation holds*

$$p^{\chi,\kappa}(t) \colon = \chi - \left(t + \kappa\left(\frac{1}{\exp(-\mathrm{St}_{\mathbf{m}_\omega}(t)) - 1} + \frac{1}{\exp(-\mathrm{St}_{\mathbf{m}_\omega}(t)) + 1}\right)\right) = 0. \tag{6.3}$$

Proof. Let t be a solution to (6.3). Let us express $\mathrm{St}_{\mathbf{m}_\omega}(t))$ from this equation. We find that

$$\mathrm{St}_{\mathbf{m}_\omega}(t) = \log(z_{\pm}(\chi,\kappa)(t)).$$

Picking the right sign we find $z(t)$ which solves (4.1). A direct computations shows that if (z,t) is a solution of 4.1 then t is a solution to (6.3).

□

Note that from Theorem 4.1 it follows that there exists a unique solution $t \in \mathbb{H}$ of (6.3). Denote

$$S(t) \colon = \mathrm{St}_{\mathbf{m}_\omega}(t)$$

for convenience.

The next Proposition defines a homeomorphism between the liquid region and the upper half-plane $\mathbb{H}$.

Proposition 6.2. *Let*

$$T_{\mathcal{L}} \colon \mathcal{L} \to \mathbb{H}$$

map $(\chi,\kappa) \in \mathcal{L}$ to the corresponding unique root of (6.3) in $\mathbb{H}$. Then, $T_{\mathcal{L}}$ is a homeomorphism with inverse $t \to (\chi_{\mathcal{L}}(t), \kappa_{\mathcal{L}}(t))$ for all $t \in \mathbb{H}$, given by

$$\chi_{\mathcal{L}}(t) = t + \frac{\exp(S(\bar{t}))(\exp(2S(t)) - 1)(t - \bar{t})}{(\exp(S(t)) - \exp(S(\bar{t})))(1 + \exp(S(t) + S(\bar{t})))}; \tag{6.4}$$

$$\kappa_{\mathcal{L}}(t) = -\frac{(\exp(2S(t)) - 1)(\exp(2S(\bar{t})) - 1)(t - \bar{t})}{2(\exp(S(t)) - \exp(S(\bar{t})))(1 + \exp(S(t) + S(\bar{t})))}. \tag{6.5}$$

Proof. The proof is completely analogous to the proof of Theorem 2.1 in [15]. For the reader's convenience we will present it.

We need to show

(1) $\mathcal{L}$ is non-empty. More precisely, we will show that whenever $|t|$ is large enough $t \to (\chi_{\mathcal{L}}(t), \kappa_{\mathcal{L}}(t)) \in \mathcal{R}$ and (6.3) holds.

(2) $\mathcal{L}$ is open.
(3) $T_{\mathcal{L}}\colon \mathcal{L} \to \mathbb{H}$ is continuous.
(4) $T_{\mathcal{L}}\colon \mathcal{L} \to \mathbb{H}$ is injective.
(5) $T_{\mathcal{L}}\colon \mathcal{L} \to T_{\mathcal{L}}(\mathcal{L})$ has inverse for all $t \in T_{\mathcal{L}}(\mathcal{L})$.
(6) $T_{\mathcal{L}}(\mathcal{L}) = \mathbb{H}$.

Let us start with (1). Fix $t \in \mathbb{H}$ and define

$$(\chi, \kappa) = (\chi_{\mathcal{L}}(t), \kappa_{\mathcal{L}}(t)) \tag{6.6}$$

using (6.4) and (6.5) . Then the following equation holds

$$(\exp(2S(t)) - 1)(t - \chi) = 2\exp(S(t))\kappa. \tag{6.7}$$

It is equivalent to (6.3).

Second, let us look at the Taylor expansions for $\chi_{\mathcal{L}}(t)$ and $\kappa_{\mathcal{L}}(t)$, when $|t|$ goes to infinity.

Let $a, b \in \mathbb{R}$ be such that Support$(\mathbf{m}_\omega) \subset [a, b]$. We have the following asymptotics for the Stieltjes transform

$$S(t) = \frac{1}{t} + \frac{\alpha}{t^2} + \frac{\beta}{t^3} + O(|t|^{-4}),$$

where $\alpha = \int_a^b x\ \mathbf{m}_\omega[dx]$ and $\beta = \int_a^b x^2 \mathbf{m}_\omega[dx]$. After some computation we get

$$\chi = \alpha + O(|t|^{-1}) \text{ and } \kappa = 1 + \left(\alpha^2 - \beta - \frac{1}{6}\right)\frac{1}{|t|^2} + O(|t|^{-3}).$$

Recall that by our assumptions $\mathbf{m}_\omega$ is a probability measure such that $b - a > 1$ since $\mathbf{m}_\omega \leqslant \lambda$, where λ is the Lebesgue measure. Therefore, we have

$$a + \frac{1}{2} = \int_a^{a+1} x dx < \alpha < \int_{b-1}^{b} x dx = b - \frac{1}{2}.$$

Similarly,

$$\beta - \alpha^2 > \frac{1}{2}\int\int_0^1 (x - y)^2 dx dy = \frac{1}{12}.$$

It follows that $(\chi, \kappa) \in (a + \frac{1}{2}, b - \frac{1}{2}) \times (0, 1)$ whenever $|t|$ is chosen to be sufficiently large. This proves (1).

Consider (2). Let $(\chi_1, \kappa_1) \in \mathcal{L}$ and $t_1 = T_{\mathcal{L}}(\chi_1, \kappa_1)$. We will show that $(\chi_2, \kappa_2) \in \mathcal{L}$ whenever $|\chi_1 - \chi_2|$ and $|\kappa_1 - \kappa_2|$ are sufficiently small. Fix $\epsilon > 0$ such that $B(t_1, \epsilon) \subset \mathbb{H}$. Let t_1 is the unique root of $p^{\chi_1,\kappa_1}(t)$ in $\mathbb{H}$, the extreme value theorem gives,

$$\inf_{t \in \partial B(t_1,\epsilon)} |p^{\chi_1,\kappa_1}(t)| > 0.$$

Also,

$$|p^{\chi_1,\kappa_1}(t) - p^{\chi_2,\kappa_2}(t)| < \epsilon \tag{6.8}$$

for any $\epsilon > 0$, whenever $|\chi_1 - \chi_2|$ and $|\kappa_1 - \kappa_2|$ are sufficiently small.

Whenever $|\chi_1 - \chi_2|$ and $|\kappa_1 - \kappa_2|$ are sufficiently small $|p^{\chi_1,\kappa_1}(t)| > |p_+^{\chi_1,\kappa_1}(t) - p_+^{\chi_2,\kappa_2}(t)|$. Rouchés Theorem implies that $p_+^{\chi_1,\kappa_1}(t)$ has a root in $B(t, \epsilon)$.

Consider (3). The analysis is very similar to part (2) and is tautologically the same as in [15].

Consider (4). Suppose there exist $(\chi_1, \kappa_1), (\chi_2, \kappa_2) \in \mathcal{L}$ such that $T_{\mathcal{L}}(\chi_1, \kappa_1) = T_{\mathcal{L}}(\chi_2, \kappa_2) = t \in \mathbb{H}$.

From 6.3 we get

$$t = \frac{\kappa_1\chi_1 - \kappa_2\chi_2}{\kappa_1 - \kappa_2}.$$

But then $t \in \mathbb{R}$ whenever $\kappa_1 \neq \kappa_2$, which contradicts $t \in \mathbb{H}$. Thus, $\kappa_1 = \kappa_2 \in (0, 1)$. It follows $\chi_1 = \chi_2$ too.

Consider (5). This follows from (6.7).

Consider (6). We already know that $T_{\mathcal{L}}(\mathcal{L})$ is open and homeomorphic to $\mathcal{L}$. Suppose there exists $t \in \partial T_{\mathcal{L}}(\mathcal{L})$ such that $t \in \mathbb{H} \backslash T_{\mathcal{L}}(\mathcal{L})$. Let $\{t_n\} \in T_{\mathcal{L}}(\mathcal{L})$ be a sequence that converges to t as $n \to \infty$. There exists a subsequence of $\{(\chi_{\mathcal{L}}(t_n), \kappa_{\mathcal{L}}(t_n))\}$ that converges to some (χ, κ). Then we can pass to the limit in (6.3) and we see that $(\chi, \kappa) \in \mathcal{R}$ and $t = T_{\mathcal{L}}(\chi, \kappa)$. This is a contradiction. □

6.2. **Gaussian Free Field.** A *Gaussian family* is a collection of Gaussian random variables $\{\xi_a\}_{a\in\Upsilon}$ indexed by an arbitrary set Υ. We assume that all our random variables are centered, that is

$$\mathbf{E}\xi_u = 0, \qquad \text{for all } u \in \Upsilon.$$

Any Gaussian family gives rise to a *covariance kernel* $\mathrm{Cov} : \Upsilon \times \Upsilon \to \mathbb{R}$ defined by

$$\mathrm{Cov}(u_1, u_2) = \mathbf{E}(\xi_{u_1}\xi_{u_2}).$$

Assume that a function $\tilde{C} : \Upsilon \times \Upsilon \to \mathbb{R}$ is such that for any $n \geqslant 1$ and $u_1, \ldots, u_n \in \Upsilon$, $[\tilde{C}(u_i, u_j)]_{i,j=1}^n$ is a symmetric and positive-definite matrix. Then there exists a centered Gaussian family with the covariance kernel $\tilde{C}$ (see e.g. [9]).

Let C_0^∞ be the space of smooth real–valued compactly supported test functions on the upper half-plane $\mathbb{H}$. Let us set

$$\tilde{G}(z, w) := -\frac{1}{2\pi} \ln \left| \frac{z - w}{z - \bar{w}} \right|, \qquad z, w \in \mathbb{H}.$$

This is the Green function of the Laplace operator on $\mathbb{H}$ with Dirichlet boundary conditions. Define a function $C : C_0^\infty \times C_0^\infty \to \mathbb{R}$ via

$$C(f_1, f_2) := \int_{\mathbb{H}} \int_{\mathbb{H}} f_1(z) f_2(w) \tilde{G}(z, w) dz d\bar{z} dw d\bar{w}.$$

The *Gaussian Free Field* (GFF) $\mathfrak{G}$ on $\mathbb{H}$ with zero boundary conditions can be defined as a Gaussian family $\{\xi_f\}_{f\in C_0^\infty}$ with covariance kernel C. The field $\mathfrak{G}$ cannot be defined as a random function on $\mathbb{H}$. However, one can make sense of the integrals $\int f(z)\mathfrak{G}(z)dz$ over finite contours in $\mathbb{H}$ with continuous functions $f(z)$, cf. [33].

6.3. **Statement of the theorem.** Consider a rectangular Aztec diamond $\mathcal{R}(N, \Omega, m)$. Let ω be a signature corresponding to the boundary row under Construction 2.7.

We have defined a probability measure P_ω^N on the sets of signatures

$$\mathcal{S}^N = (\mu^{(N)}, \nu^{(N)}, \ldots, \mu^{(1)}, \nu^{(1)}),$$

see equation (2.8).

Let us define a function Δ^N on $\mathbb{R}_{\geqslant 0} \times \mathbb{R}_{\geqslant 0} \times \mathcal{S} \to \mathbb{N}$ via

$$\Delta^N \colon (x, y, (\mu^{(N)}, \nu^{(N)}, \dots, \mu^{(1)}, \nu^{(1)})) \to \sqrt{\pi}\left|\left\{1 \leqslant sN - \lfloor y \rfloor : \mu_s^{(N-\lfloor y \rfloor)} + (N - \lfloor y \rfloor) - s \geqslant x\right\}\right|. \tag{6.9}$$

Recall the definition (3.15) of $\Delta_D^N(i,j)$, where $D \in \mathfrak{D}(N, \Omega, m)$ and (i,j) is a lattice vertex in $\mathcal{R}(N, \Omega, m)$. Its domain of definition can be extended to $(i,j) \in \mathbb{R}_{\geqslant 0} \times \mathbb{R}_{\geqslant 0}$. We get

$$\Delta^N(i, j, \mu(D)) = \sqrt{\pi}\Delta_D^N(i,j). \tag{6.10}$$

Here $\mu(D)$ is the sequence of signatures corresponding to $Y(D)$, where Y is a bijection between $\mathfrak{D}(N, \Omega, m)$ and $\mathcal{S}(N, \Omega, m)$, see Theorem 2.9.

Let us denote by $\Delta_{\mathfrak{D}}^N(x,y)$ the push-forward of the measure P_ω^N on $\mathcal{S}^N$ with respect to Δ^N. Note that due to Proposition 2.13 $\Delta_{\mathfrak{D}}^N(x,y)$ coincides with the push-forward of the uniform measure on $\mathfrak{D}(N, \Omega, m)$ with respect to Δ_D.

Let us carry $\Delta_{\mathfrak{D}}^N(x,y)$ over to $\mathbb{H}$ in the following way

$$\mathbf{\Delta}_{\mathfrak{D}}^N(z) := \Delta_{\mathfrak{D}}^N(N\chi_{\mathcal{L}}(z), N\kappa_{\mathcal{L}}(z)), \qquad z \in \mathbb{H},$$

where $\chi_{\mathcal{L}}(z)$ is defined by (6.4) and $\kappa_{\mathcal{L}}(z)$ is defined by (6.5).

For a real number $0 < \kappa < 1$ and an integer j define a moment of the random function $\mathbf{\Delta}_{\mathfrak{D}}^N$ as

$$M_j^\kappa = \int_{-\infty}^{+\infty} \chi^j \left(\mathbf{\Delta}_{\mathfrak{D}}^N(N\chi, N\kappa) - \mathbf{E}\mathbf{\Delta}_{\mathfrak{D}}^N(N\chi, N\kappa)\right) d\chi. \tag{6.11}$$

Also define the corresponding moment of GFF via

$$\mathcal{M}_j^\kappa = \int_{z \in \mathbb{H}; \kappa_{\mathcal{L}}(z) = \kappa} \chi_{\mathcal{L}}(z)^j \mathfrak{G}(z) \frac{d\chi_{\mathcal{L}}(z)}{dz} dz.$$

Theorem 6.3 (Central Limit Theorem)**.** *Let $\mathbf{\Delta}_{\mathfrak{D}}^N(z)$ be a random function corresponding to the uniformly random domino tiling of the rectangular Aztec diamond in the way described above. Then*

$$\mathbf{\Delta}_{\mathfrak{D}}^N(z) - \mathbf{E}\mathbf{\Delta}_{\mathfrak{D}}^N(z) \xrightarrow[N \to \infty]{} \mathfrak{G}(z).$$

In more details, as $N \to \infty$, the collection of random variables $\{M_j^\kappa\}_{1 \geqslant \kappa > 0; j \in \mathbb{N}}$ converges, in the sense of finitely-dimensional distributions, to $\{\mathcal{M}_j^\kappa\}_{1 \geqslant \kappa > 0; j \in \mathbb{N}}$.

Remark 6.4. *Due to Lemma 3.11 the corresponding statement for the random height function $h_{\mathfrak{D}}$ follows.*

6.4. **Schur generating functions.** For the proof we will use the moment method of Schur-generating functions from [8]. In this section we will recall necessary notions and results from [8]. After this we will apply them to our measure.

Definition 6.5. *We say that a sequence of probability measures $\rho(N)$ on $\mathbb{GT}_N$ is **CLT-appropriate** if theirs Schur generating functions $S_{\rho(N)}^{U(N)}(x_1, \dots, x_N)$ satisfy the following condition: For any fixed $k \in \mathbb{N}$ we have*

- $$\lim_{N \to \infty} \frac{\partial_i \ln S_{\rho(N)}^{U(N)}(x_1, x_2, \dots, x_k, 1^{N-k})}{N} = F(x_i), \qquad 1 \leqslant i \leqslant k,$$

•

$$\lim_{N\to\infty} \partial_i\partial_j \ln S^{U(N)}_{\rho(N)}(x_1, x_2, \dots, x_k, 1^{N-k}) = G(x_i, x_j), \qquad 1 \leqslant i, j \leqslant k,\ i \neq j,$$

where the functions $F(x)$ and $G(x, y)$ are holomorphic in a neighborhood of the unity, and the convergence is uniform over an open complex neighborhood of $(x_1, \dots, x_k) = (1^k)$. Note that the left-hand sides in these equations depend on k variables, while the right-hand sides depend on 1 or 2 variables, respectively.

For $\lambda \in \mathbb{GT}_{k_1}, \mu \in \mathbb{GT}_{k_2}$, $k_1 \geqslant k_2$, let us introduce the coefficients $\mathrm{pr}_{k_1\to k_2}(\lambda \to \mu)$ via

$$\frac{s_\lambda(x_1, \dots, x_{k_2}, 1^{k_1-k_2})}{s_\lambda(1^{k_1})} = \sum_{\mu\in\mathbb{GT}_{k_2}} \mathrm{pr}_{k_1\to k_2}(\lambda \to \mu) \frac{s_\mu(x_1, \dots, x_{k_2})}{s_\mu(1^{k_2})}.$$

The branching rule for Schur functions (see (2.7)) gives explicit values for the coefficients $\mathrm{pr}_{k_1\to k_2}(\lambda \to \mu)$.

For a symmetric function $g(x_1, \dots, x_N)$ we define the coefficients $\mathrm{st}^{(N)}_{(g)}(\lambda \to \mu)$, for $\lambda \in \mathbb{GT}_N$, $\mu \in \mathbb{GT}_N$, via

$$g(x_1, \dots, x_N) \frac{s_\lambda(x_1, \dots, x_N)}{s_\lambda(1^N)} = \sum_{\mu\in\mathbb{GT}_N} \mathrm{st}^{(N)}_{(g)}(\lambda \to \mu) \frac{s_\mu(x_1, \dots, x_N)}{s_\mu(1^N)},$$

where we assume that the function $g(x_1, \dots, x_N)$ is such that the sum in the right-hand side is finite for all λ.

Let m be a positive integer and let $0 < a_1 \leqslant \dots \leqslant a_m = 1$ be reals. Let $\rho_N = \rho_{[a_m N]}$ be a CLT-appropriate measure on $\mathbb{GT}_{[a_m N]}$ with the Schur generating function S_N, and let $g_1(x_1, \dots, x_{[a_1 N]})$, $\dots$, $g_m(x_1, \dots, x_{[a_m N]})$ be a collection of Schur generating functions of some CLT-appropriate probability measures.

Let us define the probability measure on the set

$$\mathbb{GT}_{[a_m N]} \times \mathbb{GT}_{[a_m N]} \times \mathbb{GT}_{[a_{m-1} N]} \times \mathbb{GT}_{[a_{m-1} N]} \times \dots \times \mathbb{GT}_{[a_1 N]} \times \mathbb{GT}_{[a_1 N]}.$$

That is, we need to define the probability of a collection of signatures $(\mu^{(m)}, \nu^{(m)}, \mu^{(m-1)}, \nu^{(m-1)}, \dots, \mu^{(1)}, \nu^{(1)})$, where $\mu^{(i)}, \nu^{(i)}$ are signatures of length $[a_i N]$, $i = 1, 2, \dots, m$. Let us do this in the following way.

Let

$$\begin{aligned}
H^\mu_m(x_1, \dots, x_{[a_m N]}) &:= S_N(x_1, \dots, x_{[a_m N]}),\\
H^\nu_m(x_1, \dots, x_{[a_m N]}) &:= H^\mu_m(x_1, \dots, x_{[a_m N]}) g_m(x_1, \dots, x_{[a_m N]}),\\
H^\mu_{m-1}(x_1, \dots, x_{[a_{m-1} N]}) &:= H^\nu_m(x_1, \dots, x_{[a_{m-1} N]}, 1^{[a_m N]-[a_{m-1} N]}),\\
H^\nu_{m-1}(x_1, \dots, x_{[a_{m-1} N]}) &:= H^\mu_{m-1}(x_1, \dots, x_{[a_{m-1} N]}) g_{m-1}(x_1, \dots, x_{[a_{m-1} N]}),\\
&\dots\dots\dots\dots\dots\\
H^\mu_1(x_1, \dots, x_{[a_1 N]}) &:= H^\nu_2(x_1, \dots, x_{[a_2 N]}, 1^{[a_2 N]-[a_1 N]}),\\
H^\nu_1(x_1, \dots, x_{[a_1 N]}) &:= H^\mu_1(x_1, \dots, x_{[a_1 N]}) g_1(x_1, \dots, x_{[a_1 N]}),
\end{aligned}$$

Assume that the coefficients $\mathrm{st}^{[a_t N]}_{g_t}(\mu \to \nu)$, $t = 1, \dots, s$ are positive for all t, $\mu \in \mathbb{GT}_{[a_t N]}$, $\nu \in \mathbb{GT}_{[a_t N]}$ (again, we also assume that the linear decomposition which defines these coefficients is finite).

We define the probability of the configuration $(\mu^{(m)}, \nu^{(m)}, \dots, \mu^{(1)}, \nu^{(1)})$ by

$$\begin{aligned}(6.12)\quad &\mathrm{Prob}(\mu^{(m)}, \nu^{(m)}, \mu^{(m-1)}, \nu^{(m-1)}, \dots, \mu^{(1)}, \nu^{(1)}) \\ &:= \rho_N(\mu^{(m)})\mathrm{st}_{g_1}^{[a_1N]}(\mu^{(1)} \to \nu^{(1)}) \prod_{i=2}^{m} \mathrm{st}_{g_i}^{[a_iN]}(\mu^{(i)} \to \nu^{(i)})\mathrm{pr}_{[a_iN]\to[a_{i-1}N]}(\nu^{(i)} \to \mu^{(i-1)}).\end{aligned}$$

The conditions above guarantee the existence of the following limits:

$$\lim_{N\to\infty} \frac{\partial_i \ln H_t^{\mu}(x_1, x_2, \dots, x_k, 1^{N-k})}{N} = F_t(x_i), \qquad 1 \leqslant i \leqslant k$$

$$\lim_{N\to\infty} \partial_i\partial_j \ln H_t^{\mu}(x_1, x_2, \dots, x_k, 1^{N-k}) = G_t(x_i, x_j), \qquad 1 \leqslant i, j \leqslant k,\ i \neq j,$$

for any $t = 1, 2, \dots, m$.

Let

$$p_{k;t} := \sum_{i=1}^{[a_tN]} \left(\mu_i^{(t)} + [a_tN] - i\right)^k,$$

be (shifted) moments of these signatures. These functions become random when we consider the random sequence $(\mu^{(m)}, \nu^{(m)}, \dots, \mu^{(1)}, \nu^{(1)})$ distributed according to the probability measure P_ω^N . We are interested in the asymptotic behaviour of these functions.

Theorem 6.6. ([8]) *In the notations above, the collection of random functions*

$$\{N^{-k}(p_{k;t} - \mathbf{E}p_{k;t})\}_{t=1,\dots,m;k\in\mathbb{N}}$$

is asymtoticaly Gaussian with the limit covariance

$$\begin{aligned}\lim_{N\to\infty} N^{-k_1-k_2}\mathrm{cov}\,(p_{k_1;t_1}, p_{k_2;t_2}) = \frac{a_1^{k_1}a_2^{k_2}}{(2\pi\mathbf{i})^2} \oint_{|z|=\varepsilon} \oint_{|w|=2\varepsilon} &\left(\frac{1}{z} + 1 + (1+z)F_{t_1}(1+z)\right)^{k_1} \\ \times \left(\frac{1}{w} + 1 + (1+w)F_{t_2}(1+w)\right)^{k_2} &\left(G_{t_2}(z,w) + \frac{1}{(z-w)^2}\right) dzdw,\end{aligned}$$

where $\varepsilon \ll 1$ and $1 \leqslant t_1 \leqslant t_2 \leqslant m$.

Now we will apply this theorem to our case. Consider $N \to \infty$ asymptotics of a rectangular Aztec diamond $\mathcal{R}(N, \Omega(N), m(N))$. We assume that the sequence of signatures $\omega(N)$ corresponding to the first row is regular and the sequence of measures $\{m[\omega(N)]\}$ weakly converge to $\mathbf{m}_\omega$. Our probability measure on the set of domino tilings $\mathfrak{D}(N, \Omega, m)$ defined by (2.8) has ρ concentrated on a single signature (but with a non-trivial asymptotic behavior), and the functions g_i are equal to the powers of $\prod_i(1 + x_i)$ times a constant.

We will need the following theorem.

Theorem 6.7 ([19], [8])**.** *Suppose that $\lambda(N) \in \mathbb{GT}_N$, $N = 1, 2, \dots$ is a regular sequence of signatures such that*

$$\lim_{N\to\infty} m[\lambda(N)] = \mathbf{m}.$$

Then we have

$$\lim_{N\to\infty} \partial_1\partial_2 \log\left(\frac{s_{\lambda(N)}(x_1,x_2,\dots,x_k,1^{N-k})}{s_{\lambda(N)}(1^N)}\right) = \partial_1\partial_2 \log\left(1-(x_1-1)(x_2-1)\frac{x_1H'_{\mathbf{m}}(x_1)-x_2H'_{\mathbf{m}}(x_2)}{x_1-x_2}\right), \tag{6.13}$$

where the convergence is uniform over an open complex neighborhood of $(x_1,\dots,x_k)=(1^k)$.

Construction 2.7 assigns to each row with number $[2\kappa N]$ of $\mathcal{R}(N,\Omega,m)$ a Young diagram given by a $[(1-\kappa)N]$-tuple $\mu_i^{([(1-\kappa)N])}=(\mu_1,\dots,\mu_{[(1-\kappa)N]})$. We define the moment function as

$$p_j^\kappa := \sum_{i=1}^{[(1-\kappa)N]} \left(\mu_i^{([(1-\kappa)N])}+[(1-\kappa)N]-i\right)^j.$$

Theorem 6.8. *In the notations above, the collection of random functions*

$$\{N^{-k}(p_j^\kappa-\mathbf{E}p_j^\kappa)\}_{0<\kappa\leqslant 1;j\in\mathbb{N}}$$

is asymtoticaly Gaussian with the limit covariance

$$\lim_{N\to\infty} N^{-j_2-j_1}\operatorname{cov}\left(p_{j_1}^{\kappa_1},p_{j_2}^{\kappa_2}\right) = \frac{(1-\kappa_1)^{j_1}(1-\kappa_2)^{j_2}}{(2\pi\mathbf{i})^2}\oint_{|z|=\varepsilon}\oint_{|w|=2\varepsilon}\left(\frac{1}{z}+1+(1+z)F_1(1+z)\right)^{j_1} \times\left(\frac{1}{w}+1+(1+w)F_2(1+w)\right)^{j_2}Q(z,w)dzdw, \tag{6.14}$$

where $\varepsilon\ll 1$ *and* $1\geqslant\kappa_1\geqslant\kappa_2>0$,

$$F_1(z)=\frac{1}{1-\kappa_1}\mathbf{H}'_{\mathbf{m}_\omega}(1+z)+\frac{\kappa_1}{(1-\kappa_1)(z+2)},$$

$$F_2(w)=\frac{1}{1-\kappa_2}\mathbf{H}'_{\mathbf{m}_\omega}(1+w)+\frac{\kappa_2}{(1-\kappa_2)(w+2)}$$

and

$$Q(z,w)=\partial_z\partial_w\left(\log\left(1-zw\frac{(1+z)\mathbf{H}'_{\mathbf{m}_\omega}(1+z)-(1+w)\mathbf{H}'_{\mathbf{m}_\omega}(1+w)}{z-w}\right)\right)+\frac{1}{(z-w)^2}.$$

Proof. It immediately follows from Theorem 6.6 and Lemma 3.7.

□

Remark 6.9. *Let us make several comments about this result.*

The general mechanism of Theorem 6.6 automatically produces the central limit theorem for moments. However, a further analysis is necessary in order to "extract information" from these moments and prove the convergence to the Gaussian Free Field.

In this paper we do not attempt to consider the most general classes of examples, instead, we are focused on the analysis of one specific interesting case, namely uniformly random tilings of rectangular Aztec diamonds. However, let us mention several other models where the analysis will be very similar.

First, one can use another generator of the semigroup with respect to the quantized free convolution(see Remark 3.9). In the case of rectangular Aztec diamonds we used $\prod_i(1+x_i)/2=\prod_i(1+\frac{1}{2}(x_i-1))$*, which can be understood as an extreme beta character with parameter* $\frac{1}{2}$*. Instead, one can use formulas* $\prod(1+\beta(x_i-1))$ *or* $\prod(1+\alpha(x_i-1))^{-1}$*, where* $0<\beta<1$*, and* $0<\alpha<+\infty$*. One can immediately generalise our results to the case when the probability measure comes from these formulas.*

Second, one can analyze another types of processes, in particular, Schur processes (or ensembles of nonintersecting paths, see Section 2.3). In this case one needs to suitably modify Theorem 6.6; these generalisations quite straightforwardly follow from the technique of [8]*. After this, one can apply the technique of this paper in order to extract all necessary information about limit shapes, frozen boundary, and global fluctuations.*

Finally, let us remark that while the moment method proved to be very convenient for the study of the global behavior of our model, it does not give insight on the local behavior. Nevertheless, it is possible to extract some information about it from the known results on lozenge tilings. Namely, our construction shows that the probability distribution at one level of our particle system can be viewed as a distribution at some level of uniformly random lozenge tilings of certain domains with random boundary conditions. Then the technique of [31] *and* [18] *allows to deduce the convergence to the discrete sine kernel in the bulk of this one level distribution. This approach does not provide the two-dimensional local behavior, though.*

6.5. **Proof of Theorem 6.3.** The goal of this section is to obtain Theorem 6.3 from Theorem 6.8.

First, let us make a change of variables

$$\tilde{z}=S^{(-1)}_{\mathbf{m}_\omega}\left(\log(1+z)\right),\qquad \tilde{w}=S^{(-1)}_{\mathbf{m}_\omega}\left(\log(1+w)\right),$$

in equation (6.14).

Using the connection between $S_{\mathbf{m}_\omega}(z)$ and $\mathbf{H}'_{\mathbf{m}_\omega}(z)$ (see (3.6)), we have

$$\frac{1}{z}+1+\frac{(1+z)\mathbf{H}'_{\mathbf{m}_\omega}(z+1)}{1-\kappa_1}=\frac{1}{1-\kappa_1}\left(\frac{1}{\tilde{z}}+\frac{\kappa_1}{\exp(-S_{\mathbf{m}_\omega}(\tilde{z}))-1}\right),$$
$$\frac{1}{w}+1+\frac{(1+w)\mathbf{H}'_{\mathbf{m}_\omega}(w+1)}{1-\kappa_2}=\frac{1}{1-\kappa_2}\left(\frac{1}{\tilde{w}}+\frac{\kappa_2}{\exp(-S_{\mathbf{m}_\omega}(\tilde{w}))-1}\right),$$
$$\log\left(\left(\frac{1}{w}+1+(1+w)\mathbf{H}'_{\mathbf{m}_\omega}(w)\right)-\left(\frac{1}{z}+1+(1+z)\mathbf{H}'_{\mathbf{m}_\omega}(z)\right)\right)=\log\left(\frac{1}{\tilde{w}}-\frac{1}{\tilde{z}}\right).$$

Substituting these equalities and slightly transforming the expression, we obtain that the right-hand side of (6.14) is equal to

$$\frac{1}{(2\pi\mathbf{i})^2}\oint_{|z|=\varepsilon}\oint_{|w|=2\varepsilon}\left(\frac{1}{\tilde{z}}+\frac{\kappa_1}{\exp(-S_{\mathbf{m}_\omega}(\tilde{z}))-1}+\frac{\kappa_1}{\exp(-S_{\mathbf{m}_\omega}(\tilde{z}))+1}\right)^{j_1}$$
$$\times\left(\frac{1}{\tilde{w}}+\frac{\kappa_2}{\exp(-S_{\mathbf{m}_\omega}(\tilde{w}))-1}+\frac{\kappa_2}{\exp(-S_{\mathbf{m}_\omega}(\tilde{w}))+1}\right)^{j_2}\frac{1}{(\tilde{z}-\tilde{w})^2}d\tilde{z}d\tilde{w}. \tag{6.15}$$

For any $0 < \kappa \leqslant 1$ the set $\{z \in \mathbb{H} : \kappa_{\mathcal{L}}(z) = \kappa\}$ is a well-defined curve in $\mathbb{H}$. Let $\mathcal{Z}_\kappa$ be a union of this curve and its complex conjugate.

Let $0 < \kappa_1 \leqslant \kappa_2 \leqslant 1$. Given the explicit formulae (6.4) and (6.5), it is easy to check that the curve $\mathcal{Z}_{\kappa_2}$ encircles the curve $\mathcal{Z}_{\kappa_1}$. Therefore, we can deform contours in (6.15) and obtain

$$\frac{1}{(2\pi\mathbf{i})^2} \oint\limits_{\tilde{z}\in\mathcal{Z}(\kappa_1)} \oint\limits_{\tilde{w}\in\mathcal{Z}(\kappa_2)} \left(\frac{1}{\tilde{z}} + \frac{\kappa_1}{\exp(-S_{\mathbf{m}}(\tilde{z})) - 1} + \frac{\kappa_1}{\exp(-S_{\mathbf{m}_\omega}(\tilde{z})) + 1}\right)^{j_1} \times \left(\frac{1}{\tilde{w}} + \frac{\kappa_2}{\exp(-S_{\mathbf{m}_\omega}(\tilde{w})) - 1} + \frac{\kappa_2}{\exp(-S_{\mathbf{m}_\omega}(\tilde{w})) + 1}\right)^{j_2} \frac{1}{(\tilde{z}-\tilde{w})^2} d\tilde{z}d\tilde{w}. \tag{6.16}$$

Note that for $\tilde{z} \in \mathcal{Z}(\kappa_1)$ the expression

$$\frac{1}{\tilde{z}} + \frac{\kappa_1}{\exp(-S_{\mathbf{m}_\omega}(\tilde{z})) - 1} + \frac{\kappa_1}{\exp(-S_{\mathbf{m}_\omega}(\tilde{z})) + 1}$$

is real and is equal to $\chi_{\mathcal{L}}(z)$, see Lemma 6.1. Therefore, we can rewrite (6.16) as

$$-\frac{1}{4\pi^2} \oint\limits_{\tilde{z}\in\mathcal{Z}(\kappa_1)} \oint\limits_{\tilde{w}\in\mathcal{Z}(\kappa_2)} \chi_{\mathcal{L}}(\tilde{z})^{j_1} \chi_{\mathbf{m}}(\tilde{w})^{j_2} \frac{1}{(\tilde{z}-\tilde{w})^2} d\tilde{z}d\tilde{w},$$

Integrating (6.11) by parts we see that

$$M_j^\kappa = \frac{N^{-j+1}\sqrt{\pi}}{j+1} \left(p_{j+1}^\kappa - \mathbf{E}p_{j+1}^\kappa\right).$$

Therefore, the set $\{M_j^\kappa\}_{1\geqslant\kappa>0, j\in\mathbb{N}}$ converges to the Gaussian distribution with zero mean and limit covariance

$$\lim_{N\to\infty} \operatorname{cov}\left(M_{j_1}^{\kappa_1}, M_{j_1}^{\kappa_1}\right) = \frac{-1}{4\pi(j_1+1)(j_2+1)} \oint\limits_{z\in\mathcal{Z}(\kappa_1)} \oint\limits_{z\in\mathcal{Z}(\kappa_2)} \chi_{\mathcal{L}}(z)^{j_1} \chi_{\mathcal{L}}(z)^{j_2} \times \frac{d\chi_{\mathcal{L}}(z)}{dz} \frac{d\chi_{\mathcal{L}}(w)}{dw} \frac{1}{(z-w)^2} dzdw. \tag{6.17}$$

By definition, the set $\{\mathcal{M}_j^\kappa\}_{1\geqslant\kappa>0, j\in\mathbb{N}}$ is Gaussian with zero mean and covariance

$$\operatorname{cov}\left(\mathcal{M}_{j_1}^{\kappa_1}, \mathcal{M}_{j_2}^{\kappa_2}\right) = \oint\limits_{z\in\mathbb{H}:\kappa_{\mathcal{L}}(z)=\kappa_1} \oint\limits_{z\in\mathbb{H}:\kappa_{\mathcal{L}}(z)=\kappa_2} \chi_{\mathcal{L}}(z)^{j_1} \chi_{\mathcal{L}}(z)^{j_2} \times \frac{d\chi_{\mathcal{L}}(z)}{dz} \frac{d\chi_{\mathcal{L}}(w)}{dw} \left(\frac{-1}{2\pi} \ln\left|\frac{z-w}{z-\bar{w}}\right|\right) dzdw. \tag{6.18}$$

Using the equality

$$2\ln\left|\frac{z-w}{z-\bar{w}}\right| = \ln(z-w) - \ln(z-\bar{w}) - \ln(\bar{z}-w) + \ln(\bar{z}-\bar{w}),$$

we can write it in the form

$$\operatorname{cov}\left(\mathcal{M}_{j_1}^{\kappa_1}, \mathcal{M}_{j_2}^{\kappa_2}\right) = -\frac{1}{4\pi} \oint\limits_{z\in\mathcal{Z}(\kappa_1)} \oint\limits_{z\in\mathcal{Z}(\kappa_2)} \chi_{\mathbf{m}}(z)^{j_1} \chi_{\mathbf{m}}(z)^{j_2} \frac{d\chi_{\mathbf{m}}(z)}{dz} \frac{d\chi_{\mathbf{m}}(w)}{dw} \ln(z-w) dzdw.$$

Integration by parts shows that this formula coincides with the right-hand side of (6.17) which concludes the proof of the theorem.

7. Examples of the frozen boundary

Consider $N \to \infty$ asymptotics such that all the dimensions of a rectangular Aztec diamond $\mathcal{R}(N, \Omega(N), m(N))$ linearly grow with N. We assume that the sequence of signatures $\omega(N)$ corresponding to the first row is regular and $\lim\limits_{N\to\infty} m[\omega(N)] = \mathbf{m}_\omega$. We will start with a general description of a part of the boundary called the *edge*.

For a set $R \subset \mathbb{R}$ let $\bar{R}$ denote its closure and R° denote its interior. Following [15] we can show that

$$(\chi_{\mathcal{L}}(\cdot), \kappa_{\mathcal{L}}(\cdot))\colon \mathbb{H} \to \mathcal{L}$$

difined by (6.4) and (6.5) has a unique continuous extension to the open set $R \subset \mathbb{R}$ given by,

$$R\colon = \left(\overline{(\mathbb{R}\backslash \mathrm{Supp}(\mathbf{m}_\omega)) \cup (\mathbb{R}\backslash \mathrm{Supp}(\lambda - \mathbf{m}_\omega))}\right)^\circ, \tag{7.1}$$

where λ denotes the Lebesgue measure (recall that under the assumptions above $\mathbf{m}_\omega$ is absolutely continious with respect to Lebesgue measure with the density $\leqslant 1$). This is a direct consequence of Lemma 2.2 in [15]. The extension is denoted by $(\chi_{\mathcal{E}}(\cdot), \kappa_{\mathcal{E}}(\cdot))$. We conclude that $(\chi_{\mathcal{E}}(t), \kappa_{\mathcal{E}}(t))$ for all $t \in R$ belongs to the frozen boundary and $(\chi_{\mathcal{E}}(\cdot), \kappa_{\mathcal{E}}(\cdot))\colon \mathbb{H} \to \partial\mathcal{L}$ is a smooth curve parametrised over R, moreover, this map is injective. We will also call this curve the *edge* and denote it $\mathcal{E}$.

The set R can be represented in the following way

$$\mathbb{R} = (\mathbb{R}\backslash \mathrm{Supp}(\mathbf{m}_\omega)) \cup (\mathbb{R}\backslash \mathrm{Supp}(\lambda - \mathbf{m}_\omega)) \cup R_1 \cup R_2,$$

where

- R_1 is the set of all $t \in \mathbb{R}$ for which there exist an $\epsilon > 0$ with $(t, t+\epsilon) \subset \mathbb{R}\backslash \mathrm{Supp}(\mathbf{m}_\omega)$ and $(t-\epsilon, t) \subset \mathbb{R}\backslash \mathrm{Supp}(\lambda - \mathbf{m}_\omega)$.
- R_2 is the set of all $t \in \mathbb{R}$ for which there exist an $\epsilon > 0$ with $(t, t+\epsilon) \subset (\mathbb{R}\backslash \mathrm{Supp}(\lambda - \mathbf{m}_\omega))$ and $(t-\epsilon, t) \subset (\mathbb{R}\backslash \mathrm{Supp}(\mathbf{m}_\omega))$.

Proposition 7.1. *Denote $S(t) := \mathrm{St}_{\mathbf{m}_\omega}(t)$. A point $\chi_{\mathcal{E}}(t), \kappa_{\mathcal{E}}(t))$ belongs to the frozen boundary $\partial\mathcal{L}$ for all $t \in (\mathbb{R}\backslash \mathrm{Supp}(\mathbf{m}_\omega)) \cup (\mathbb{R}\backslash \mathrm{Supp}(\lambda - \mathbf{m}_\omega))$, where*

$$\chi_{\mathcal{E}}(t) = t + \frac{(\exp(2S(t)) - 1)}{S'(t)(1 + \exp(2S(t)))} \text{ and } \kappa_{\mathcal{E}}(t) = -\frac{(\exp(2S(t)) - 1)^2}{2\exp(S(t))S'(t)(1 + \exp(2S(t)))}. \tag{7.2}$$

Fix $t \in R_1$. Let $I_1 = (t_2, t_1)$ be an interval with $t \in I_1$ such that $(t, t_1) \subset \mathbb{R}\backslash Supp(\mathbf{m}_\omega)$ and $(t_2, t) \subset \mathbb{R}\backslash Supp(\lambda - \mathbf{m}_\omega)$. Denote $S_{I_1}(t) = \int\limits_{\mathbb{R}\backslash I_1} \frac{\mathbf{m}_\omega[dx]}{t-x}$. Then $(\chi_{\mathcal{E}}(t), \kappa_{\mathcal{E}}(t)) \in \partial\mathcal{L}$, where

$$\chi_{\mathcal{E}}(t) = t - \exp\left(S_{I_1}(t)\right)(t - t_2) \text{ and } \kappa_{\mathcal{E}}(t) = 0. \tag{7.3}$$

Fix $t \in R_2$. Let $I_2 = (t_2, t_1)$ be an interval with $t \in I_1$ such that $(t, t_1) \subset \mathbb{R} \backslash Supp(\lambda - \mathbf{m}_\omega)$ and $(t_2, t) \subset \mathbb{R} \backslash Supp(\mathbf{m}_\omega)$. Denote $S_{I_2}(t) = \int\limits_{\mathbb{R}\backslash I_2} \frac{\mathbf{m}_\omega[dx]}{t-x}$. Then $(\chi_{\mathcal{E}}(t), \kappa_{\mathcal{E}}(t)) \in \partial\mathcal{L}$, where

$$\chi_{\mathcal{E}}(t) = t \text{ and } \kappa_{\mathcal{E}}(t) = -\frac{1}{2}\exp\left(-S_{I_2}(t)\right)(t - t_1). \tag{7.4}$$

The result is independent of the choice of I_1, I_2.

Proof. The statement follows from Lemma 2.2 [15]. The proof repeats the arguments in Lemma 2.3 [15]. □

Note that the above fomulas (7.2) agree with our computations for the rectangular Aztec diamonds of type (N, A^s, B^s), see the proof of the Theorem 5.1.

7.1. **The Aztec diamond.** The Aztec diamond is a rectangular Aztec diamond of type $(N, A^1 = 1, B^1 = N)$. In this case we have $a_1 = 0$ and $b_1 = 1$.

Therefore, we obtain

$$\mathrm{St}_{\mathbf{m}_\omega}(t) = \log\frac{t}{t-1}.$$

Then we solve the equation $\mathrm{St}_{\mathbf{m}_\omega}(t) = \log z$ for t and substitute it into (4.2) we get

$$F_\kappa(z) = \frac{z}{z-1} + \frac{\kappa z}{(1-\kappa)(z+1)}.$$

Solving explicitly the equation

$$F_\kappa(z) = \frac{\chi}{1-\kappa}$$

we find

$$\mathbf{z}_+^\kappa(\chi) = \frac{-1 + 2\kappa + \sqrt{(2\chi-1)^2 + (2\kappa-1)^2 - 1}}{2(1-\chi)}.$$

Thus, the density

$$d\mathbf{m}^\kappa\left(\frac{\chi}{1-\kappa}\right) = \frac{1}{\pi}\mathrm{Arg}\left(\frac{-1 + 2\kappa + \sqrt{(2\chi-1)^2 + (2\kappa-1)^2 - 1}}{2(\chi-1)}\right),$$

where (χ, κ) is such that $(2\chi-1)^2 + (2\kappa-1)^2 - 1 < 0$.

Thus, the frozen boundary is given by equation

$$(2\chi-1)^2 + (2\kappa-1)^2 - 1 = 0,$$

as expected.

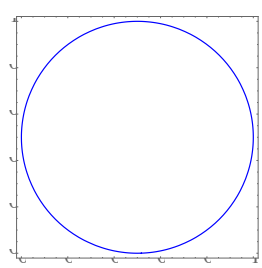

FIGURE 17. The Arctic circle.

7.2. **The Aztec half-diamond.**

Definition 7.2. *The Aztec half-diamond is a rectangular Aztec diamond* $\mathcal{R}(N, \Omega, N-1)$, *where* $\Omega = (1, 3, \ldots, 2N-1)$.

Note that that the number of blocks of consecutive unit squares in the boundary row grows with infinity. Thus, the results from Chapter 5 are not directly applicable here.

This domain was considered in [30]. We obtain that $\mathbf{m}_\omega$ is a uniform measure on $[0, 2]$. In this case we can again explicitly compute

$$\mathrm{St}_{\mathbf{m}_\omega}(t) = -\frac{1}{2}\log\sqrt{1-\frac{2}{t}}.$$

Then we solve the equation $\mathrm{St}_{\mathbf{m}_\omega}(t) = \log z$ for t and substitute it into (4.2) we get

$$F_\kappa(z) = \frac{2z(\kappa - z)}{(-1+z)(1+z)} = \chi.$$

Therefore,

$$d\mathbf{m}^\kappa\left(\frac{\chi}{1-\kappa}\right) = \frac{1}{\pi}\mathrm{Arg}\left(\frac{-\kappa + \sqrt{\kappa^2 + \chi(\chi-2)}}{\chi - 2}\right).$$

So the frozen boundary is given by the equation

$$\kappa^2 + \chi(\chi - 2) = 0.$$

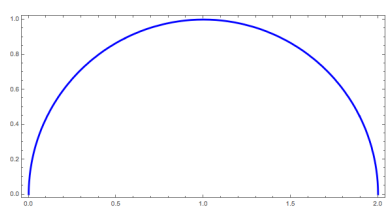

FIGURE 18. The frozen boundary for a uniform measure on $[0, 2]$.

7.3. **Aztec half-diamond with parameters** (θ, N)**..**

Definition 7.3. *The Aztec half-diamond diamond with parameters* (θ, N) *is a rectangular Aztec diamond* $\mathcal{R}(N, \Omega, (\theta-1)(N-1))$, *where* $\Omega = (1, 1+\theta, \ldots, \theta(N-1)+1)$.

Let $\theta = 4$. We obtain that $\mathbf{m}_\omega$ is a uniform measure on $[0, 4]$. In this case we can again explicitly compute

$$\mathrm{St}_{\mathbf{m}_\omega}(t) = -\frac{1}{4}\log\sqrt{1-\frac{4}{t}}.$$

We can still explicitly solve the system (6.1) on the computer and we encounter the following expression under the square root:

$$f(\chi, \kappa) = 27\kappa^4 + (\kappa^2 + (\chi - 4)\chi)^3.$$

Then the frozen boundary is given by this equation.

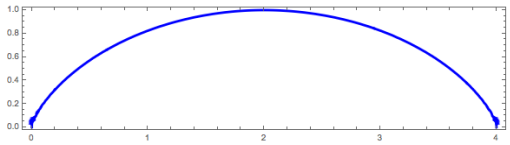

FIGURE 19. The frozen boundary for a uniform measure on $[0, 4]$.

We see that for this class of the examples the frozen boundary will still be an algebraic curve (or a subset of an algebraic curve more generally.) Meanwhile, when $\mathrm{St}_{\mathbf{m}_\omega}(t)$ is no longer a logarithm of a rational function the frozen boundary may not be algebraic anymore. This follows from (7.2).

REFERENCES

[1] G. Anderson, A. Guionnet, O. Zeitouni, An introduction to random matrices, *Cambridge Studies in Advanced Mathematics*, vol 118, Cambridge University Press.

[2] D. Betea, C. Boutillier, J. Bouttier, G. Chapuy, S. Corteel, M. Vuletic, Perfect sampling algorithms for Schur processes, Preprint (2015), `http://arxiv.org/pdf/1407.3764.pdf`.

[3] A. Borodin , S. Shlosman, Gibbs Ensembles of Nonintersecting Paths *Comm. in Math. Physics*. January 2010, 293:145, `http://arxiv.org/pdf/0804.0564v1.pdf`.

[4] A. Borodin, P.L. Ferrari, Random tilings and Markov chains for interlacing particles, Preprint (2015), `http://arxiv.org/pdf/1506.03910v1.pdf`.

[5] J. Bouttier, G. Chapuy, S. Corteel, From Aztec diamonds to pyramids: steep tilings, Preprint, (2014), `http://arxiv.org/abs/1407.0665`.

[6] C. Boutillier, J. Bouttier, G. Chapuy, S. Corteel, and S. Ramassamy, Dimers on Rail Yard Graphs, Preprint, (2015), `http://arxiv.org/abs/1504.05176`.

[7] A. Bufetov, V. Gorin, Representations of classical Lie groups and quantized free convolution, *Geometric and Functional Analysis*, June 2015, Volume 25, Issue 3, pp 763-814, `http://arxiv.org/pdf/1311.5780.pdf`.

[8] A. Bufetov, V. Gorin, Preprint (2016), `https://arxiv.org/pdf/1604.01110v1`.

[9] P. Cartie, Introduction a l'etude des mouvements browniens a plusieurs parametres, *Seminaire de probabilites (Strasbourg)*, 5:58–75, 1971.

[10] C. Chhita, K. Johansson, Domino statistics of the two-periodic Aztec diamond, Preprint, (2014), `http://arxiv.org/pdf/1410.2385.pdf`.

[11] M. Ciucu, Perfect matchings of cellular graphs, *J. Algebraic Combin.*, 5 (1996), 87–103.

[12] M. Ciucu, Enumeration of perfect matchings in graphs with reflective symmetry, *J. Comb. Theory*, Ser. A 77 (1997), 67–97.

[13] H. Cohn, N. Elkies, J. Propp, Local statistics for random domino tilings of the Aztec diamond, *Duke Math. J.*, 85 (1996), 117–166, `http://arxiv.org/pdf/math/0008243.pdf`.

[14] H. Cohn, R. Kenyon, J. Propp. A variational principle for domino tilings. *J. Amer. Math. Soc.*, 14(2):297–346 (electronic), (2001), `http://arxiv.org/pdf/math/0008220v3.pdf`.

[15] E. Duse, A. Metcalfe, Asymptotic geometry of discrete interlaced patterns:Part I, Preprint, (2015), `http://arxiv.org/abs/1412.6653`.

[16] N. Elkies, G. Kuperberg, M. Larsen, and J. Propp. Alternating-sign matrices and domino tilings I, *Journal Algebraic Combin.*, 1(2):111–132, (1992), `http://arxiv.org/pdf/math/9201305v1.pdf`.

[17] P. L. Ferrari and H. Spohn, Domino tilings and the six-vertex model at its free-fermion point, *J. Phys.* A, 39(33):10297–10306, 2006, `http://arxiv.org/pdf/cond-mat/0605406v1.pdf`.

[18] V. Gorin. Bulk universality for random lozenge tilings near straight boundaries and for tensor products, Preprint, (2016), `arXiv:1603.02707`

[19] V. Gorin, G. Panova, Asymptotics of symmetric polynomials with applications to statistical mechanics and representation theory, *Annals of Probability*, Volume 43, Number 6 (2015), 3052–3132, `http://arxiv.org/pdf/1301.0634v6.pdf`.

[20] A. Guionnet, M. Maïda, A Fourier view on the R-transform and related asymptotics of spherical integrals, *Journal of Functional Analysis*, 222 (2005), no. 2, 435–490, http://arxiv.org/pdf/math/0406121v3.pdf.

[21] W. Jochush, J. Propp, P. Shor, Random domino tilings and the arctic circle theorem, Preprint, (1995), http://arxiv.org/abs/math/9801068.

[22] K. Johansson. The arctic circle boundary and the Airy process, *Annals of Probability*, 33(1):1–30, 2005, http://arxiv.org/pdf/math/0306216.pdf.

[23] K. Johansson, Non-intersecting paths, random tilings and random matrices, *Probab. Theory Related Fields*, 123, 225–280, 2002, http://arxiv.org/pdf/math/0011250v1.pdf.

[24] R. Kenyon, Dominos and the Gaussian free field, *Annals of Probability* ,29 (2001), 1128–1137, http://arxiv.org/pdf/math-ph/0002027.pdf.

[25] R. Kenyon. Height fluctuations in the honeycomb dimer model, *Comm. Math. Phys.*, 281 (2008) 675–709, http://arxiv.org/pdf/math-ph/0405052v2.pdf.

[26] R. Kenyon. Lectures on dimers, 2009, http://www.math.brown.edu/Ëœrkenyon/papers/dimerlecturenotes.pdf.

[27] R. Kenyon, A. Okounkov, Limit shapes and the complex Burgers equation, *Acta Mathematica,* December 2007, Volume 199, Issue 2, pp 263-302, http://arxiv.org/pdf/math-ph/0507007v3.pdf.

[28] W. H. Mills, D. P. Robbins, and H. Rumsey, Alternating sign matrices and descending plane partitions, *J. Comb. Theory Ser.* A 34 (1983), 340–359.

[29] A. Nica, R. Speicher, Lectures on the Combinatorics of Free Probability, *Cambridge University Press*, 2006.

[30] E. Nordenstam,, B. Young. Domino shuffling on Novak half-hexagons and Aztec half-diamonds. *Electronic J. Combin.,* 18(1), Paper 181, 22, 2011, http://arxiv.org/pdf/1103.5054.pdf.

[31] L. Petrov. Asymptotics of Random Lozenge Tilings via Gelfand-Tsetlin Schemes, *Probability Theory and Related Fields*, 160 (2014), no. 3, 429–487, http://arxiv.org/pdf/1202.3901v2.pdf.

[32] L. Petrov. Asymptotics of Uniformly Random Lozenge Tilings of Polygons. Gaussian Free Field, *Annals of Probability*, 43 (2014), no. 1, 1–43, http://arxiv.org/pdf/1206.5123.pdf

[33] S. Sheffield, Gaussian free fields for mathematicians, *Probability Theory and Related Fields*, 139:521–541, 2007, http://arxiv.org/pdf/math/0312099v3.pdf.

[34] J.R. Stembridge, Nonintersecting paths, Pfaffians, and plane partitions, *Adv. Math.*, 83 (1990), 96–131.

[35] D. Voiculescu, K. Dykema, A. Nica, Free random variables, *CRM Monograph Series*, vol. 1, American Mathematical Society, Providence, RI, 1992.

[36] H. Weyl, The Classical Groups:Their invariants and representations. Princeton, University Press, 1939.

(Alexey Bufetov) Department of Mathematics, Massachusetts Institute of Technology, Cambridge, MA, USA. E-mail: alexey.bufetov@gmail.com

(Alisa Knizel) Department of Mathematics, Massachusetts Institute of Technology, Cambridge, MA, USA. E-mail: alisik@math.mit.edu